Wishart Random Matrices in Probabilistic Structural Mechanics

Sondipon Adhikari[1]

Abstract: Uncertainties need to be taken into account for credible predictions of the dynamic response of complex structural systems in the high and medium frequency ranges of vibration. Such uncertainties should include uncertainties in the system parameters and those arising due to the modeling of a complex system. For most practical systems, the detailed and complete information regarding these two types of uncertainties is not available. In this paper, the Wishart random matrix model is proposed to quantify the total uncertainty in the mass, stiffness, and damping matrices when such detailed information regarding uncertainty is unavailable. Using two approaches, namely, (a) the maximum entropy approach; and (b) a matrix factorization approach, it is shown that the Wishart random matrix model is the simplest possible random matrix model for uncertainty quantification in discrete linear dynamical systems. Four possible approaches for identifying the parameters of the Wishart distribution are proposed and compared. It is shown that out of the four parameter choices, the best approach is when the mean of the inverse of the random matrices is same as the inverse of the mean of the corresponding matrix. A simple simulation algorithm is developed to implement the Wishart random matrix model in conjunction with the conventional finite-element method. The method is applied vibration of a cantilever plate with two different types of uncertainties across the frequency range. Statistics of dynamic responses obtained using the suggested Wishart random matrix model agree well with the results obtained from the direct Monte Carlo simulation.

DOI: 10.1061/(ASCE)0733-9399(2008)134:12(1029)

CE Database subject headings: Matrix methods; Parameters; Estimation; Vibration; Structural response.

Introduction

The equation of motion of a damped n degree of freedom linear structural dynamical system can be expressed as

$$\mathbf{M}\ddot{\mathbf{q}}(t) + \mathbf{C}\dot{\mathbf{q}}(t) + \mathbf{K}\mathbf{q}(t) = \mathbf{f}(t) \tag{1}$$

where $\mathbf{f}(t) \in \mathbb{R}^n$=forcing vector; $\mathbf{q}(t) \in \mathbb{R}^n$=response vector; and $\mathbf{M} \in \mathbb{R}^{n\times n}$, $\mathbf{C} \in \mathbb{R}^{n\times n}$, and $\mathbf{K} \in \mathbb{R}^{n\times n}$=mass, damping, and stiffness matrices, respectively. When uncertainties exist in the system parameters, boundary conditions and geometry are considered, and the system matrices become random matrices. Uncertainties in Eq. (1) are completely characterized by the joint probability density function of the random matrices $\mathbf{M}$, $\mathbf{C}$, and $\mathbf{K}$. There are two approaches to obtain the probability density functions of the system matrices. The first is the *parametric approach* and the second is the *nonparametric approach*. In the parametric approach, the uncertainties associated with the system parameters, such as Young's modulus, mass density, Poisson's ratio, damping coefficient, and geometric parameters are quantified using statistical methods. Once the uncertainties are quantified, the response of the system can be obtained using the stochastic finite-element method; see for example, Shinozuka and Yamazaki (1998), Ghanem and Spanos (1991), Kleiber and Hien (1992), Matthies et al. (1997), Manohar and Adhikari (1998a,b), Adhikari and Manohar (1999, 2000), Haldar and Mahadevan (2000), Sudret and Der-Kiureghian (2000), Nair and Keane (2002), Elishakoff and Ren (2003), and Sachdeva et al. (2006a,b). This type of approach is suitable for data/aleatoric uncertainties. Epistemic/model uncertainties on the other hand do not explicitly depend on the system parameters. For example, there can be unquantified errors associated with the equation of motion (linear or nonlinear), in the damping model (viscous or nonviscous), in the model of structural joints, and also in the numerical methods (e.g., discretization of displacement fields, truncation and round-off errors, tolerances in the optimization and iterative algorithms, step sizes in the time-integration methods). It is evident that the parametric approach is not suitable to quantify these types of uncertainties and nonparametric approaches have been proposed by Soize (2000, 2001) and Adhikari (2007a,b) for this purpose. The importance of considering parametric and/or nonparametric uncertainty also depends on the frequency of excitation. In the high-frequency vibration, the wave lengths of the vibration modes become very small and the vibration response can be very sensitive to the small details of the system. In such situations, a nonparametric approach such as the statistical energy analysis (SEA) (Lyon and Dejong 1995) can be used. On the other hand, for low-frequency vibration problems, a parametric approach such as the stochastic finite-element method is adequate. In the medium-frequency vibration problems, both parametric and nonparametric uncertainties need to be considered. We refer the readers to the works by Langley and Bremner (1999), Sarkar and Ghanem (2002, 2003a,b), Langley and Cotoni (2007), and Cotoni et al. (2007) for discussions on midfrequency vibration analysis in linear dynamical systems.

In the majority of practical problems, the complete informa-

[1]Chair of Aerospace Engineering, School of Engineering, Swansea Univ., Singleton Park, Swansea SA2 8PP, U.K.

Note. Associate Editor: Arvid Naess. Discussion open until May 1, 2009. Separate discussions must be submitted for individual papers. The manuscript for this paper was submitted for review and possible publication on December 18, 2006; approved on November 28, 2007. This paper is part of the ***Journal of Engineering Mechanics***, Vol. 134, No. 12, December 1, 2008. ©ASCE, ISSN 0733-9399/2008/12-1029–1044/ $25.00.

tion regarding uncertainties is not available. In some cases, for example, cars manufactured from a production chain and soil property distribution in a construction site, it may be possible to obtain probabilistic descriptions of the system parameters experimentally. However, obtaining such probabilistic information may be prohibitively expensive for many problems. In another class of problems, for example, dynamic analysis of a space vehicle, even "in principle" it may not be possible to obtain probabilistic information because there may be just "only one sample." However, there will still be some uncertainties in the model. Regardless of what type of uncertainties exist in the model of a linear dynamical system as given by Eq. (1), it must be characterized by the random matrices $\mathbf{M}$, $\mathbf{C}$, and $\mathbf{K}$. These random matrices, therefore, can be used to model both parametric and nonparametric uncertainty in the system. Motivated by this observation, in this paper we obtain the probability density function of the random matrices based on a parameter estimation point of view. It is first shown that the Wishart random matrix is the simplest physically realistic random matrix model for the system matrices appearing in linear structural dynamical systems. Four different physically realistic parameter selection approaches are discussed and compared using numerical examples. Based on the numerical results, the best method among the four proposed methods is identified.

Matrix Variate Probability Density Functions

In this section, the concept of matrix variate probability density functions or random matrices is introduced. A random matrix can be considered as an observable phenomenon representable in the form of a matrix, which under repeated observation, yields different nondeterministic outcomes. Therefore, a random matrix is simply a collection of random variables that may satisfy certain rules (for example, symmetry, positive definiteness, etc.). Random matrices were introduced by Wishart (1928) in the context of multivariate statistics. However, the random matrix theory (RMT) was not used in other branches until the 1950s when Wigner (1958) published his works (leading to the Nobel prize in Physics in 1963) on the eigenvalues of random matrices arising in high-energy physics. Using an asymptotic theory for large dimensional matrices, Wigner was able to bypass the Schrödinger equation and explain the statistics of measured atomic energy levels in terms of the limiting eigenvalues of these random matrices. Since then, research on random matrices has continued to attract interest in multivariate statistics, physics, number theory, and more recently in mechanical and electrical engineering. We refer the reader to the books by Mezzadri and Snaith (2005), Tulino and Verdú (2004), Eaton (1983), Girko (1990), Muirhead (1982), and Mehta (1991) for the history and applications of random matrix theory.

The probability density function of a random matrix can be defined in a manner similar to that of a random variable or random vector. See the book by Gupta and Nagar (2000, p. 44) for a more formal definition of random matrices. If $\mathbf{A}$ is a $n\times m$ real random matrix, then the matrix variate probability density function of $\mathbf{A}\in\mathbb{R}^{n\times m}$, denoted by $p_{\mathbf{A}}(\mathbf{A})$, is a mapping from the space of $n\times m$ real matrices to the real line, i.e., $p_{\mathbf{A}}(\mathbf{A}):\mathbb{R}^{n\times m}\rightarrow\mathbb{R}$. Here, we define the probability density functions of few random matrices, which are relevant to stochastic mechanics problems.

Gaussian random matrix. A rectangular random matrix $\mathbf{X}\in\mathbb{R}^{n\times p}$ is said to have a matrix variate Gaussian distribution with the mean matrix $\mathbf{M}\in\mathbb{R}^{n\times p}$ and the covariance matrix $\mathbf{\Sigma}\otimes\mathbf{\Psi}$, where $\mathbf{\Sigma}\in\mathbb{R}_n^+$ and $\mathbf{\Psi}\in\mathbb{R}_p^+$ provided the pdf of $\mathbf{X}$ is given by

$$p_{\mathbf{X}}(\mathbf{X}) = (2\pi)^{-np/2}|\mathbf{\Sigma}|^{-p/2}|\mathbf{\Psi}|^{-n/2} \times \mathrm{etr}\left\{-\frac{1}{2}\mathbf{\Sigma}^{-1}(\mathbf{X}-\mathbf{M})\mathbf{\Psi}^{-1}(\mathbf{X}-\mathbf{M})^T\right\} \quad (2)$$

This distribution is usually denoted as $\mathbf{X}\sim N_{n,p}\ (\mathbf{M},\mathbf{\Sigma}\otimes\mathbf{\Psi})$

Symmetric Gaussian random matrix. Let $\mathbf{Y}\in\mathbb{R}^{n\times n}$ be a symmetric random matrix and $\mathbf{M}$, $\mathbf{\Sigma}$, and $\mathbf{\Psi}$ are $n\times n$ constant matrices such that the commutative relation $\mathbf{\Sigma\Psi}=\mathbf{\Psi\Sigma}$ holds. If the $n(n+1)/2\times 1$ vector $\mathrm{vecp}(\mathbf{Y})$ formed from $\mathbf{Y}$ is distributed as $N_{n(n+1)/2,1}\ (\mathrm{vecp}(\mathbf{M}),\mathbf{B}_n^T(\mathbf{\Sigma}\otimes\mathbf{\Psi})\mathbf{B}_n)$, then $\mathbf{Y}$ is said to have a symmetric matrix variate Gaussian distribution with mean $\mathbf{M}$ and covariance matrix $\mathbf{B}_n^T(\mathbf{\Sigma}\otimes\mathbf{\Psi})\mathbf{B}_n$ and its pdf is given by

$$p_{\mathbf{Y}}(\mathbf{Y}) = (2\pi)^{-n(n+1)/4}|\mathbf{B}_n^T(\mathbf{\Sigma}\otimes\mathbf{\Psi})\mathbf{B}_n|^{-1/2} \times \mathrm{etr}\left\{-\frac{1}{2}\mathbf{\Sigma}^{-1}(\mathbf{Y}-\mathbf{M})\mathbf{\Psi}^{-1}(\mathbf{Y}-\mathbf{M})^T\right\} \quad (3)$$

This distribution is usually denoted as $\mathbf{Y}=\mathbf{Y}^T\sim SN_{n,n}\ (\mathbf{M},\mathbf{B}_n^T(\mathbf{\Sigma}\otimes\mathbf{\Psi})\mathbf{B}_n)$.

For a symmetric matrix $\mathbf{Y}\in\mathbb{R}^{n\times n}$, $\mathrm{vecp}(\mathbf{Y})$ is a $n(n+1)/2$-dimensional column vector formed from the elements above and including the diagonal of $\mathbf{Y}$ taken columnwise. The elements of the translation matrix $\mathbf{B}_n\in\mathbb{R}^{n^2\times n(n+1)/2}$ are given by

$$(B_n)_{ij,gh} = \frac{1}{2}(\delta_{ig}\delta_{jh}+\delta_{ih}\delta_{jg}) \quad i\leqslant n, j\leqslant n, g\leqslant h\leqslant n \quad (4)$$

where δ_{ij}=usual Kronecker's delta.

Wishart matrix. A $n\times n$ symmetric positive definite random matrix $\mathbf{S}$ is said to have a Wishart distribution with parameters $p\geqslant n$ and $\mathbf{\Sigma}\in\mathbb{R}_n^+$, if its pdf is given by

$$p_{\mathbf{S}}(\mathbf{S}) = \left\{2^{(1/2)np}\Gamma_n\left(\frac{1}{2}p\right)|\mathbf{\Sigma}|^{(1/2)p}\right\}^{-1}|\mathbf{S}|^{(1/2)(p-n-1)}\mathrm{etr}\left\{-\frac{1}{2}\mathbf{\Sigma}^{-1}\mathbf{S}\right\} \quad (5)$$

This distribution is usually denoted as $\mathbf{S}\sim W_n(p,\mathbf{\Sigma})$.

Matrix variate gamma distribution. A $n\times n$ symmetric positive definite random matrix $\mathbf{W}$ is said to have a matrix variate gamma distribution with parameters a and $\mathbf{\Psi}\in\mathbb{R}_n^+$, if its pdf is given by

$$p_{\mathbf{W}}(\mathbf{W}) = \{\Gamma_n(a)|\mathbf{\Psi}|^{-a}\}^{-1}|\mathbf{W}|^{a-(1/2)(n+1)}\mathrm{etr}\{-\mathbf{\Psi W}\} \qquad \Re(a)>\frac{1}{2}(n-1) \quad (6)$$

This distribution is usually denoted as $\mathbf{W}\sim G_n(a,\mathbf{\Psi})$. The matrix variate gamma distribution was used by Soize (2000, 2001) for the random system matrices of linear dynamical systems.

In Eqs. (5) and (6), the function $\Gamma_n(a)$=multivariate gamma function, which can be expressed in terms of products of the univariate gamma functions as

$$\Gamma_n(a) = \pi^{(1/4)n(n-1)}\Pi_{k=1}^n\Gamma\left[a-\frac{1}{2}(k-1)\right] \quad \text{for } \Re(a)>\frac{1}{2}(n-1) \quad (7)$$

For more details on the matrix variate distributions, we refer the reader to the books by Tulino and Verdú (2004), Gupta and Nagar (2000), Eaton (1983), Muirhead (1982), Girko (1990),

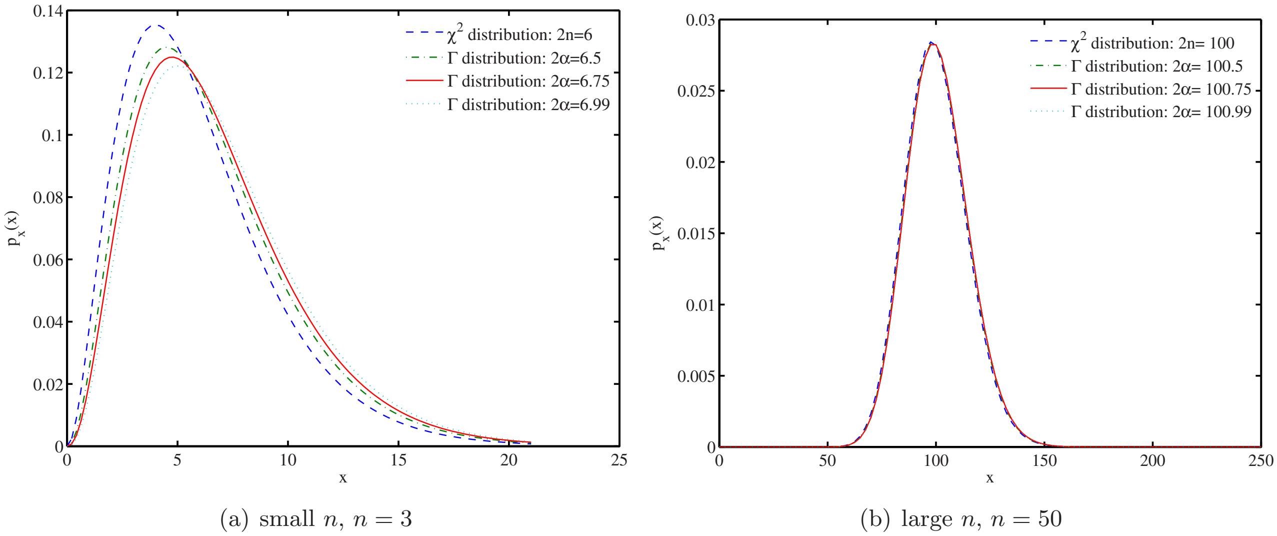

Fig. 1. Comparison between equivalent chi-square and gamma random variables appearing respectively in the diagonals of Wishart and gamma random matrices

and references therein. Among the four types of random matrices introduced above, the distributions given by Eqs. (5) and (6) will always result in symmetric and positive definite matrices. Therefore, they can be possible candidates for modeling random system matrices arising in probabilistic structural dynamics.

Comparing the gamma distribution with the Wishart distribution, we have $G_n(a,\mathbf{\Psi})=W_n(2a,\mathbf{\Psi}^{-1}/2)$. The main difference between the gamma and the Wishart distribution is that originally only integer values were considered for the shape parameter p in the Wishart distribution. It is a misconception that p is limited to integer numbers. One can easily observe that Eq. (5) is valid for all real p greater than n [when $p<n$, then the distribution is often called the anti-Wishart distribution, see Janik and Nowak (2003)]. Therefore, from an analytical point of view, the gamma and the Wishart distributions are identical. However, a difference arises when ensembles are digitally simulated as the diagonals of a gamma matrix are gamma random variables whereas in the case of a Wishart matrix they are chi-square random variables. For large matrices, as expected in structural dynamics applications, the difference between chi-square random variables and gamma random variables is negligible. If the dimensions of the matrix are n, the diagonal entries of the Wishart matrix would be chi-square random variables with at least n degree of freedom. For a gamma random matrix, the diagonals would be gamma random variables with shape parameters α equal to at least $n/2$, and $\beta=2$ [see Johnson et al. (1994), p. 338]. In Fig. 1, equivalent chi-square and gamma random variables appearing, respectively, in the diagonals of Wishart and gamma random matrices are compared.

When the value of n is small ($n=3$ is used for illustration), from Fig. 1(a) it can be observed that a chi-square random variable is different from the gamma random variables with close fractional values. However, when n is large ($n=50$ is used for illustration), as expected in structural dynamic applications, from Fig. 1(b) it can be observed that there is very little difference between a chi-square random variable and gamma random variables with close fractional values. This numerical result shows that numerically there is very little difference between Wishart and gamma random matrices when they are large. As a result, only Wishart random matrices will be considered in this paper.

Probability Density Functions of the System Matrices

In this section, two approaches are discussed to obtain the matrix variate distributions of the random system matrices $\mathbf{M}$, $\mathbf{C}$, and $\mathbf{K}$. The first approach is based on the maximum entropy principle and the second approach is based on the factorization of random matrices.

Pdf of the Random System Matrices Using the Maximum Entropy Approach

Soize (2000, 2001) used this approach to obtain the probability density functions of the system matrices. Suppose that the mean values of $\mathbf{M}$, $\mathbf{C}$, and $\mathbf{K}$ are given by $\bar{\mathbf{M}}$, $\bar{\mathbf{C}}$, and $\bar{\mathbf{K}}$, respectively. The matrix variate distributions of the random system matrices should be such that

a. $\mathbf{M}$, $\mathbf{C}$, and $\mathbf{K}$ are symmetric matrices;
b. $\mathbf{M}$ is positive definite and $\mathbf{C}$ and $\mathbf{K}$ are nonnegative-definite matrices; and
c. The moments of the inverse of the dynamic stiffness matrix

$$\mathbf{D}(\omega)=-\omega^2\mathbf{M}+i\omega\mathbf{C}+\mathbf{K} \tag{8}$$

should exist $\forall\omega$. That is, if $\mathbf{H}(\omega)$=frequency response function (FRF) matrix, given by

$$\mathbf{H}(\omega)=\mathbf{D}^{-1}(\omega)=[-\omega^2\mathbf{M}+i\omega\mathbf{C}+\mathbf{K}]^{-1} \tag{9}$$

then the following condition must be satisfied:

$$\mathrm{E}[\|\mathbf{H}(\omega)\|_{\mathrm{F}}^{\nu}]<\infty \qquad \forall\ \omega \tag{10}$$

Here, ν=order of the inverse-moment constraint. For example, if $\mathbf{H}(\omega)$ is considered to be a second-order (matrix variate) random process, then $\nu=2$ should be used. This constraint is clearly arising from the fact that the moments and the pdf of the response vector must exist for all frequencies of excitation. Because the matrices $\mathbf{M}$, $\mathbf{C}$, and $\mathbf{K}$ have similar probabilistic characteristics, for notational convenience we will use the notation $\mathbf{G}$, which stands for any one of the system matrices. Suppose the matrix variate density function of $\mathbf{G} \in \mathbb{R}_n^+$ is given by $p_{\mathbf{G}}(\mathbf{G}): \mathbb{R}_n^+ \to \mathbb{R}$. We have the following information and constraints to obtain $p_{\mathbf{G}}(\mathbf{G})$:

$$\int_{\mathbf{G}>0} p_{\mathbf{G}}(\mathbf{G}) d\mathbf{G} = 1 \quad \text{(the normalization)} \tag{11}$$

and

$$\mathrm{E}[\mathbf{G}] = \int_{\mathbf{G}>0} \mathbf{G} p_{\mathbf{G}}(\mathbf{G}) d\mathbf{G} = \bar{\mathbf{G}} \quad \text{(the mean matrix)} \tag{12}$$

The mean matrix $\bar{\mathbf{G}}$ is symmetric and positive definite and the integrals appearing in these equations are $n(n+1)/2$ dimensional.

The exact application of the constraint that the inverse moments of the dynamic stiffness matrix should exist for all frequencies requires the derivation of the joint probability density function of the random matrices $\mathbf{M}$, $\mathbf{C}$, and $\mathbf{K}$. This problem is extremely difficult to treat analytically. Therefore, we consider a simpler problem where it is required that the inverse moments of each of the system matrices $\mathbf{M}$, $\mathbf{C}$, and $\mathbf{K}$ must exist. Provided the system is damped, this condition will always guarantee the existence of the moments of the frequency response function matrix. This is only a *sufficient condition* and not a necessary condition. As a result, except the stiffness matrix (to take account of the static case when $\omega=0$), the distributions arising from this approach will be more constrained than what is necessary.

Maximizing the entropy associated with the matrix variate probability density function $p_{\mathbf{G}}(\mathbf{G})$

$$\mathcal{S}(p_{\mathbf{G}}) = -\int_{\mathbf{G}>0} p_{\mathbf{G}}(\mathbf{G}) \ln\{p_{\mathbf{G}}(\mathbf{G})\} d\mathbf{G} \tag{13}$$

and using the constraints in Eqs. (11) and (12), it can be shown that (Soize 2000, 2001) the maximum-entropy pdf of $\mathbf{G}$ follows the Wishart distribution with parameters $p=(2\nu+n+1)$ and $\boldsymbol{\Sigma}=\bar{\mathbf{G}}/(2\nu+n+1)$, that is $\mathbf{G} \sim \mathbf{W}_n\,(2\nu+n+1, \bar{\mathbf{G}}/(2\nu+n+1))$. The maximum-entropy approach not only gives the form of the pdf of the system matrices, but also its parameters.

Pdf of the Random System Matrices Using the Matrix Factorization Approach

In this section, an alternative approach is discussed to obtain the probability density function of the random system matrices. Because $\mathbf{G}$ is a symmetric and positive-definite random matrix, it can always be factorized as

$$\mathbf{G} = \mathbf{X}\mathbf{X}^T \tag{14}$$

where $\mathbf{X} \in \mathbb{R}^{n \times p}$; and $p \geqslant n$ is in general a rectangular matrix. Since the factorization in Eq. (14) will always guarantee the satisfaction of the symmetry and the positive-definiteness condition, we consider that this is *the* form of the random system matrices arising in structural dynamics. Now we need to study the probabilistic nature of the random matrix $\mathbf{X}$. Once the pdf of $\mathbf{X}$ is known, the pdf $\mathbf{G}$ can be derived using the nonlinear matrix transformation in Eq. (14). The simplest case is when the mean of $\mathbf{X}$ is $\mathbf{O} \in \mathbb{R}^{n \times p}$, $p \geqslant n$ and the covariance tensor of $\mathbf{X}$ is given by $\boldsymbol{\Sigma} \otimes \mathbf{I}_p \in \mathbb{R}^{np \times np}$ where $\boldsymbol{\Sigma} \in \mathbb{R}_n^+$. Following Gupta and Nagar (2000, Chap. 3), it can be shown that if $\mathbf{X} \sim N_{n,p}(\mathbf{O}, \boldsymbol{\Sigma} \otimes \mathbf{I}_p)$, then the pdf of $\mathbf{G}$ in Eq. (14) is a Wishart distribution so that $\mathbf{G} \sim W_n(p, \boldsymbol{\Sigma})$ as given in Eq. (5) (see Appendix I for details). How to obtain p and $\boldsymbol{\Sigma}$ will be discussed later in the paper.

Statistical Properties of the Wishart Random Matrices and Their Inverse

In the previous section using two different approaches, it was shown that each system matrix follows a Wishart distribution. The maximum entropy approach gives the form of the distribution (Wishart/gamma) as well as its parameters, whereas the matrix factorization approach only gives the form of the distribution. The rest of the paper is mainly devoted to parameter identification of the Wishart distribution.

The use of the Wishart distribution in the context of structural dynamics turns out to be very useful because it has been studied extensively in the multivariate statistics literature; see for example, the books by Muirhead (1982), Eaton (1983), Gupta and Nagar (2000), and Mathai and Provost (1992). In this section, we consider some statistical properties of the Wishart random matrix and its inverse, which are crucial for the parameter identification problem.

Assuming that $\mathbf{G}$ has the Wishart distribution with parameters $p=\theta+n+1$ and $\boldsymbol{\Sigma}=\bar{\mathbf{G}}/(\theta+n+1)$, the first moment (mean), the second moment, the elements of the covariance tensor, and the variance of $\mathbf{G}$ can be obtained following Gupta and Nagar (2000, Chap. 3) as

$$\mathrm{E}[\mathbf{G}] = p\boldsymbol{\Sigma} = \bar{\mathbf{G}} \tag{15}$$

$$\begin{aligned}\mathrm{E}[\mathbf{G}^2] = p\boldsymbol{\Sigma}^2 + p\,\mathrm{Trace}(\boldsymbol{\Sigma})\boldsymbol{\Sigma} + p^2\boldsymbol{\Sigma}^2 = \frac{1}{\theta+n+1}[(\theta+n+2)\bar{\mathbf{G}}^2 \\ + \bar{\mathbf{G}}\,\mathrm{Trace}(\bar{\mathbf{G}})]\end{aligned} \tag{16}$$

$$\mathrm{cov}(G_{ij}, G_{kl}) = p(\Sigma_{ik}\Sigma_{jl} + \Sigma_{il}\Sigma_{jk}) = \frac{1}{\theta+n+1}(\bar{G}_{ik}\bar{G}_{jl} + \bar{G}_{il}\bar{G}_{jk}) \tag{17}$$

$$\mathrm{E}[\{\mathbf{G} - \mathrm{E}[\mathbf{G}]\}^2] = \mathrm{E}[\mathbf{G}^2] - \bar{\mathbf{G}}^2 = \frac{1}{\theta+n+1}[\bar{\mathbf{G}}^2 + \bar{\mathbf{G}}\,\mathrm{Trace}(\bar{\mathbf{G}})] \tag{18}$$

It is useful to define the normalized standard deviation of $\mathbf{G}$ as

$$\sigma_G^2 = \frac{\mathrm{E}[\|\mathbf{G} - \mathrm{E}[\mathbf{G}]\|_{\mathrm{F}}^2]}{\|\mathrm{E}[\mathbf{G}]\|_{\mathrm{F}}^2} \tag{19}$$

This measure of uncertainty was introduced by Soize (2000) as the dispersion parameter. Because both $\mathrm{E}[\bullet]$ and $\mathrm{Trace}(\bullet)$ are linear operators, their order can be interchanged. Using Eqs. (15) and (16), we have

$$\begin{aligned}\mathrm{E}[\|\mathbf{G} - \mathrm{E}[\mathbf{G}]\|_{\mathrm{F}}^2] &= \mathrm{E}[\mathrm{Trace}([\mathbf{G} - \mathrm{E}[\mathbf{G}]][\mathbf{G} - \mathrm{E}[\mathbf{G}]]^T)] \\ &= \mathrm{Trace}(\mathrm{E}[[\mathbf{G}^2 - \mathbf{G}\mathrm{E}[\mathbf{G}] - \mathrm{E}[\mathbf{G}]\mathbf{G} - \mathrm{E}[\mathbf{G}]^2]]) \\ &= \mathrm{Trace}(\mathrm{E}[\mathbf{G}^2] - \mathrm{E}[\mathbf{G}]^2) \\ &= \mathrm{Trace}(p\boldsymbol{\Sigma}^2 + p\,\mathrm{Trace}(\boldsymbol{\Sigma})\boldsymbol{\Sigma} + p^2\boldsymbol{\Sigma}^2 - (p\boldsymbol{\Sigma})^2) \\ &= p\,\mathrm{Trace}(\boldsymbol{\Sigma}^2) + p\{\mathrm{Trace}(\boldsymbol{\Sigma})\}^2\end{aligned} \tag{20}$$

Therefore

$$\sigma_G^2 = \frac{p\,\mathrm{Trace}(\boldsymbol{\Sigma}^2) + p\{\mathrm{Trace}(\boldsymbol{\Sigma})\}^2}{p^2\mathrm{Trace}(\boldsymbol{\Sigma}^2)} = \frac{1}{p}\left\{1 + \frac{\{\mathrm{Trace}(\boldsymbol{\Sigma})\}^2}{\mathrm{Trace}(\boldsymbol{\Sigma}^2)}\right\}$$
$$= \frac{1}{\theta + n + 1}\left\{1 + \frac{\{\mathrm{Trace}(\bar{\mathbf{G}})\}^2}{\mathrm{Trace}(\bar{\mathbf{G}}^2)}\right\} \tag{21}$$

Eq. (21) shows that the normalized standard deviation of $\mathbf{G}$ will be smaller for higher values of θ. This implies that for a system with a fixed dimension, the uncertainty in the system matrices reduces when θ increases. Recall that θ is the order of the inverse moment that we have enforced to exist. Intuitively, Eq. (21) implies that if we enforce more constraints (in terms of the order of the inverse moment), the resulting distribution becomes less uncertain. This fact, in turn, allows one to control the amount of uncertainty in the system by choosing different values of θ. It is interesting to observe that the parameter θ, which was originally used as the order of the inverse-moment constraint, now solely controls the amount of variability in the matrices as both n and $\bar{\mathbf{G}}$ are fixed. If σ_G^2 is known (e.g., from experiments, stochastic finite-element calculations or experience) then Eq. (21) can be used to calculate θ. Next, we consider the properties of the inverse of the system matrices.

Suppose $\mathbf{F}=\mathbf{G}^{-1}$ denotes the inverse of a system matrix. The Jacobian of this transformation is given by Mathai (1997) as $J(\mathbf{G}\to\mathbf{F})=|\mathbf{F}|^{-(n+1)}$. Using this, the pdf of the inverse of the system matrices can be obtained. The inverse of a Wishart matrix is also known as the inverted Wishart matrix, which is defined as follows:

Inverted Wishart matrix: a $n\times n$ symmetric positive definite matrix random $\mathbf{V}$ is said to have an inverted Wishart distribution with parameters m and $\boldsymbol{\Psi}\in\mathbb{R}_n^+$, if its pdf is given by

$$p_{\mathbf{V}}(\mathbf{V}) = \frac{2^{-(1/2)(m-n-1)n}|\boldsymbol{\Psi}|^{(1/2)(m-n-1)}}{\Gamma_n\left(\frac{1}{2}(m-n-1)\right)|\mathbf{V}|^{m/2}}\mathrm{etr}\{-\mathbf{V}^{-1}\boldsymbol{\Psi}\} \quad m>2n \quad \boldsymbol{\Psi}>0 \tag{22}$$

This distribution is usually denoted as $\mathbf{V}\sim IW_n(m,\boldsymbol{\Psi})$. From this we can say that the inverse of a system matrix has an inverted Wishart distribution with parameters $m=\theta+2(n+1)$ and $\boldsymbol{\Psi}=(\theta+n+1)\bar{\mathbf{G}}^{-1}$. Following Gupta and Nagar (2000, Chap. 3), the first moment (mean) and the second moment can be obtained exactly in closed form as

$$\mathrm{E}[\mathbf{G}^{-1}] = \frac{\boldsymbol{\Psi}}{m-2n-2} = \frac{\theta+n+1}{\theta}\bar{\mathbf{G}}^{-1} \tag{23}$$

$$\mathrm{E}[\mathbf{G}^{-2}] = \frac{\mathrm{Trace}(\boldsymbol{\Psi})\boldsymbol{\Psi} + (m-2n-1)\boldsymbol{\Psi}^2}{(m-2n-1)(m-2n-2)(m-2n-4)}$$
$$= \frac{(\theta+n+1)^2\mathrm{Trace}(\bar{\mathbf{G}}^{-1})\bar{\mathbf{G}}^{-1} + \theta\bar{\mathbf{G}}^{-2}}{\theta(\theta+1)(\theta-2)} \tag{24}$$

From Eq. (23) observe that θ must be more than 0 for the existence of the mean of the inverse matrices. Similarly, from Eq. (24), for the existence of the second inverse moment θ must be more than 2. These values give explicit constraints for the condition that $\mathbf{G}^{-1}$ be a second-order random matrix. However, recall that except for the stiffness matrix, the condition that $\mathbf{G}^{-1}$ be a second-order random matrix is *not* a necessary condition.

Parameter Selection for the Wishart Distribution

Using two different approaches we have shown that the matrix variate pdf of the system matrices can be represented by the Wishart random matrices. Moreover, the maximum entropy approach naturally provides the parameters for the Wishart distribution. It was shown that $\mathbf{G}$ has the Wishart distribution with parameters $p=\theta+n+1$ and $\boldsymbol{\Sigma}=\bar{\mathbf{G}}/(\theta+n+1)$. These parameter selections, however, give rise to the following fundamental problem as shown in the example below.

Example 1. Suppose the degrees of freedom of a system $n=1{,}000$ and $\theta=4$. Therefore, from Eq. (15) we have $\mathrm{E}[\mathbf{G}]=\bar{\mathbf{G}}$ and from Eq. (23), we have

$$\mathrm{E}[\mathbf{G}^{-1}] = \frac{\theta+n+1}{\theta}\bar{\mathbf{G}}^{-1} = \frac{4+1{,}000+1}{4}\bar{\mathbf{G}}^{-1} = 251.25\bar{\mathbf{G}}^{-1} \tag{25}$$

This implies that the mean of the inverse of the matrix is 251.25 times more than the inverse of the mean matrix.

This is clearly nonphysical for engineering structural matrices because the randomness of a real system is not very large. One possible way to reduce this "gap" is to increase the value of θ. However, this implies the reduction of the variance, that is, the assumption of more constraints than is necessary. This discrepancy between the "mean of the inverse" and the "inverse of the mean" of the random matrices is a crucial drawback of the parameters obtained using the maximum entropy approach. A new approach based on the least-squares error minimization was proposed by Adhikari (2007a) to overcome this problem. In this paper, we compare four parameter selection options, namely, the original approach by Soize (2000, 2001), the least-squares error minimization approach by Adhikari (2007a), and two new approaches introduced in this paper.

The parameters p and $\boldsymbol{\Sigma}$ of the Wishart matrices can be obtained based on what criteria we select. For this parameter estimation problem, the "data" consist of the "measured" mean ($\bar{\mathbf{G}}$) and normalized standard deviation ($\tilde{\sigma}_G$) of a system matrix. We investigate the following four possible choices for parameter estimation:

1. *Criterion 1:* for each system matrix, we consider that the mean of the random matrix is the same as the deterministic matrix and the normalized standard deviation is the same as the measured normalized standard deviation. Mathematically this implies $\mathrm{E}[\mathbf{G}]=\bar{\mathbf{G}}$ and $\sigma_G=\tilde{\sigma}_G$. This condition results in

$$p = n+1+\theta \quad \text{and} \quad \boldsymbol{\Sigma} = \bar{\mathbf{G}}/p \tag{26}$$

where

$$\theta = \frac{1}{\tilde{\sigma}_G^2}\left\{1 + \frac{\{\mathrm{Trace}(\bar{\mathbf{G}})\}^2}{\mathrm{Trace}(\bar{\mathbf{G}}^2)}\right\} - (n+1) \tag{27}$$

This criteria was proposed by Soize (2000, 2001).

2. *Criterion 2:* for each system matrix, we consider that the mean of the random matrix and the mean of the inverse of the random matrix are closest to the deterministic matrix and its inverse. Mathematically this implies $\|\bar{\mathbf{G}}-\mathrm{E}[\mathbf{G}]\|_{\mathrm{F}}$ and $\|\bar{\mathbf{G}}^{-1}-\mathrm{E}[\mathbf{G}^{-1}]\|_{\mathrm{F}}$ are minimum and $\sigma_G=\tilde{\sigma}_G$. This condition results in

$$p = n + 1 + \theta \quad \text{and} \quad \boldsymbol{\Sigma} = \bar{\mathbf{G}}/\alpha \tag{28}$$

where $\alpha = \sqrt{\theta(n+1+\theta)}$ and θ is as defined in Eq. (27). This is known as the optimal Wishart distribution (see Appendix II for details) and was proposed by Adhikari (2007a). The rationale behind this approach is that a random system matrix and its inverse should be mathematically treated in a similar manner as both are symmetric and positive-definite matrices.

3. *Criterion 3:* here we consider that for each system matrix, the mean of the inverse of the random matrix is equal to the inverse of the deterministic matrix and the normalized standard deviation is same as the measured normalized standard deviation. Mathematically this implies $\mathrm{E}[\mathbf{G}^{-1}] = \bar{\mathbf{G}}^{-1}$ and $\sigma_G = \tilde{\sigma}_G$. Using Eq. (23) and after some simplifications one obtains

$$p = n + 1 + \theta \quad \text{and} \quad \boldsymbol{\Sigma} = \bar{\mathbf{G}}/\theta \tag{29}$$

where θ is defined in Eq. (27).

4. *Criterion 4:* these criteria arise from the idea that the mean of the eigenvalues of the distribution is the same as the "measured" eigenvalues of the mean matrix and the normalized standard deviation is the same as the measured normalized standard deviation. Mathematically we can express this as

$$\mathrm{E}[\mathbf{M}^{-1}] = \bar{\mathbf{M}}^{-1} \quad \mathrm{E}[\mathbf{K}] = \bar{\mathbf{K}} \quad \sigma_M = \tilde{\sigma}_M \quad \text{and} \quad \sigma_K = \tilde{\sigma}_K \tag{30}$$

This implies that the parameters of the mass matrix are selected according to Criterion 3 and the parameters for the stiffness matrix is selected according to Criterion 1. The damping matrix is obtained using Criterion 2. This case is, therefore, a combination of the previous three cases.

Simulation Algorithm Using Wishart System Matrices

It will be shown in the numerical examples, that among the four approaches discussed above, the Wishart random matrix corresponding to Criterion 3 produces the best results. Therefore, for all practical purposes, the random matrix model for a system matrix should be a Wishart matrix with parameters $p = n+1+\theta$ and $\boldsymbol{\Sigma} = \bar{\mathbf{G}}/\theta$. This leads to a simple and general simulation algorithm for probabilistic structural dynamics. The method can be implemented by following these steps

1. From the deterministic matrices $\bar{\mathbf{G}} \equiv \{\bar{\mathbf{M}}, \bar{\mathbf{C}}, \bar{\mathbf{K}}\}$ using the standard finite-element method. Obtain n, the dimension of the system matrices.
2. Obtain the normalized standard deviations or the "dispersion parameters" $\tilde{\sigma}_G \equiv \{\tilde{\sigma}_M, \tilde{\sigma}_C, \tilde{\sigma}_K\}$ corresponding to the system matrices. This can be obtained from experiment, experience, or using the stochastic finite-element method.
3. Calculate

$$\theta_G = \frac{1}{\tilde{\sigma}_G^2}\left\{1 + \frac{\{\mathrm{Trace}(\bar{\mathbf{G}})\}^2}{\mathrm{Trace}(\bar{\mathbf{G}}^2)}\right\} - (n+1) \quad \text{for } \mathbf{G} = \{\mathbf{M}, \mathbf{C}, \mathbf{K}\} \tag{31}$$

4. Approximate $(n+1+\theta_G)$ to its nearest integer and call it p. That is $p = [n+1+\theta_G]$. For complex engineering systems, n can be in the order of several thousands or even millions. As shown in the numerical example before, this approximation would introduce negligible error. Create a $n \times p$ matrix $\tilde{\mathbf{X}}$ with Gaussian random numbers with zero mean and unit covariance, i.e., $\tilde{\mathbf{X}} \sim N_{n,p}(\mathbf{O}, \mathbf{I}_n \otimes \mathbf{I}_p)$.
5. Because $\boldsymbol{\Sigma} = \bar{\mathbf{G}}/\theta_G$ is a positive definite matrix, it can be factorized as $\boldsymbol{\Sigma} = \boldsymbol{\Gamma}\boldsymbol{\Gamma}^T$. Using the matrix $\boldsymbol{\Gamma} \in \mathbb{R}^{n \times n}$, obtain the matrix $\mathbf{X}$ using the linear transformation

$$\mathbf{X} = \boldsymbol{\Gamma}\tilde{\mathbf{X}} \tag{32}$$

Following Theorem 2.3.10 in Gupta and Nagar (2000), it can be shown that $\mathbf{X} \sim N_{n,p}(\mathbf{O}, \boldsymbol{\Sigma} \otimes \mathbf{I}_p)$.

6. Now obtain the samples of the Wishart random matrices $W_n(n+1+\theta_G, \bar{\mathbf{G}}/\theta_G)$ as

$$\mathbf{G} = \mathbf{X}\mathbf{X}^T \tag{33}$$

Alternatively, MATLAB (The MathWorks Inc., Natick, MA) command wishrnd can be used to generate the samples of Wishart matrices. MATLAB can handle fractional values of $(n+1+\theta_G)$ so that the approximation to its nearest integer in Step 5 may be avoided.

7. Repeat the above process for the mass, stiffness, and damping matrices and solve the equation of motion for each sample to obtain the response statistics of interest.

This procedure can be implemented easily. Once the samples of the system matrices are generated, the rest of the analysis is identical to any Monte Carlo simulation-based approach. If one implements this approach in conjunction with a commercial finite-element software, unlike the stochastic finite-element method, the commercial software needs to be accessed only once to obtain the mean matrices. This simulation procedure is, therefore, "nonintrusive."

Although the random matrix-based approach outlined above is very easy to implement, there are some limitations:

- The statistical correlations between mass, stiffness, and damping matrices cannot be considered in the present form. One must derive the matrix variate joint probability density function for **M**, **K**, and **C**.
- Unlike the deterministic matrices derived from finite-element discretization, sample-wise sparsity may not be preserved for the random matrices.
- Only one variable, namely, the normalized standard deviation σ_G defined in Eq. (19), is available to characterize uncertainty in a system matrix. This can be obtained, for example using standard system identification tools (e.g., modal identification) across the ensemble.
- Unlike the parametric uncertainty quantification methods, no computationally efficient analytical method (e.g., perturbation method, polynomial chaos expansion) is yet available for the random matrix approach.

In the medium- and high-frequency vibration of stochastic systems, where there is enough "mixing" of the modes, the dynamic response is not very sensitive to the detailed nature of uncertainty in the system. In this situation, in spite of the limitations mentioned above, the random matrix approach provides an easy alternative to the conventional parametric approach. The numerical examples in the next section illustrate this fact.

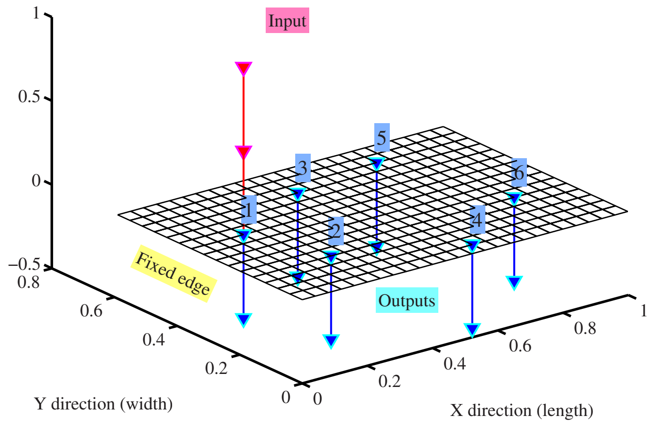

Fig. 2. Finite-element model of a steel cantilever plate: 25×15 elements, 416 nodes, 1,200 degrees of freedom, the deterministic properties are: $\bar{E}=200\times10^9\ \mathrm{N/m^2}$, $\bar{\mu}=0.3$, $\bar{\rho}=7{,}860\ \mathrm{kg/m^3}$, $\bar{t}=3.0$ mm, $L_x=0.998$ m, $L_y=0.59$ m, input node number: 481, output node numbers: 481, 877, 268, 1,135, 211, and 844, modal damping factor: 2% for all modes

Numerical Example: Dynamic Response of a Plate with Uncertainties

A cantilever steel plate with uncertain properties is considered to illustrate the application of Wishart random matrices in probabilistic structural dynamics. The diagram of the plate, together with the deterministic numerical values assumed for the system parameters are shown in Fig. 2. The plate is excited by a unit harmonic force and the response is calculated at the point shown in the diagram. The standard four-noded thin plate bending element (resulting in 12 degrees of freedom per element) is used. The plate is divided into 25 elements along the x-axis and 15 elements along the y-axis for the numerical calculations. The resulting system has 1,200 degrees of freedom so that $n=1{,}200$. A response is calculated for the six points shown in the figure. Here we show results corresponding to Points 1 and 2 only.

Two different cases of uncertainties are considered. In the first case, it is assumed that the material properties are randomly inhomogeneous. In the second case, we consider that the plate is "perturbed" by attaching spring-mass oscillators at random locations. The first case corresponds to a parametric uncertainty problem while the second case corresponds to a nonparametric uncertainty problem.

Plate with Randomly Inhomogeneous Material Properties

It is assumed that the Young's modulus, Poisson's ratio, mass density, and thickness are random fields of the form

$$E(\mathbf{x}) = \tilde{E}(1 + \epsilon_E f_1(\mathbf{x})) \tag{34}$$

$$\mu(\mathbf{x}) = \tilde{\mu}(1 + \epsilon_\mu f_2(\mathbf{x})) \tag{35}$$

$$\rho(\mathbf{x}) = \tilde{\rho}(1 + \epsilon_\rho f_3(\mathbf{x})) \tag{36}$$

$$\text{and } t(\mathbf{x}) = \bar{t}(1 + \epsilon_t f_4(\mathbf{x})) \tag{37}$$

The two-dimensional vector $\mathbf{x}$ denotes the spatial coordinates. The strength parameters are assumed to be $\epsilon_E=0.15$, $\epsilon_\mu=0.10$, $\epsilon_\rho=0.14$, and $\epsilon_t=0.12$. The random fields $f_i(\mathbf{x})$, $i=1,\ldots,4$ are assumed to be delta-correlated homogeneous Gaussian random fields. A 1,000-sample Monte Carlo simulation is performed to obtain the FRFs.

We want to identify which of the four Wishart matrix fitting approaches proposed here would produce the highest fidelity with direct stochastic finite-element Monte Carlo simulation results. From the simulated random mass and stiffness matrices, we obtain $n=1{,}200$, $\sigma_M=0.0999$, and $\sigma_K=0.2151$. Since a 2% constant modal damping factor is assumed for all the modes, $\sigma_C=0$. The *only* uncertainty related information used in the random matrix approach are the values of σ_M and σ_K. The information regarding which element property functions are random fields, nature of these random fields (correlation structure, Gaussian or non-Gaussian), and the amount of randomness are *not* used in the Wishart matrix approach. This is aimed to depict a realistic situation when the detailed information regarding uncertainties in a complex engineering system is not available to the analyst. Using $n=1{,}200$, $\sigma_M=0.0999$, and $\sigma_K=0.2151$, together with the deterministic values of $\mathbf{M}$ and $\mathbf{K}$, from Eq. (31) we obtain

$$\theta_M = 32{,}924 \text{ and } \theta_K = 5{,}777 \tag{38}$$

Using these, the samples of the mass and stiffness matrices are simulated following the procedure outlined in the previous section.

The predicted mean of the amplitude using the direct stochastic finite-element simulation and four Wishart matrix approaches are compared in Fig. 3 for the driving-point FRF.

In Figs. 3(b–d), we have separately shown the low-, medium-, and high-frequency response, obtained by zooming in the appropriate frequency ranges in Fig. 3(a). There are, of course, no fixed and definite boundaries between the low-, medium-, and high-frequency ranges. We have selected 0–0.8 kHz as the low-frequency range, 0.8–2.2 kHz as the medium-frequency range, and 2.2–4.0 kHz as the high-frequency range. These frequency boundaries are selected on the basis of the qualitative nature of the response and devised purely for the clarity in presenting the results.

In Fig. 4, percentage errors in the mean of the amplitude of the driving-point FRF obtained using the proposed four Wishart matrix approaches are shown. Percentage errors are calculated using the direct Monte Carlo simulation results as the benchmarks.

An error using any one of the random matrix approaches reduces with the increase in the frequency. Among the four Wishart matrix approaches discussed here, Approach 3, that is when the mean of the inverse is the same as the inverse of the mean matrix, produces the least error across the frequency range. Moreover, Approach 3 is significantly more accurate in the low-frequency region compared to the other approaches.

The predicted standard deviation of the amplitude using the direct stochastic finite-element simulation and four Wishart matrix approaches are compared in Fig. 5 for the driving-point FRF. In Figs. 5(b–d), we have separately shown the low-, medium-, and high-frequency response, obtained by zooming in the appropriate frequency ranges in Fig. 5(a). The overall features of these plots are similar to the mean results shown before.

In Fig. 6, percentage errors in the standard deviation of the amplitude of the driving-point FRF obtained using the proposed four Wishart matrix approaches are shown. Like the mean, error in standard deviation using any one the random matrix approaches reduces with the increase in the frequency. Among the four Wishart matrix approaches discussed here, Approach 3, that is when the mean of the inverse is the same as the inverse of the

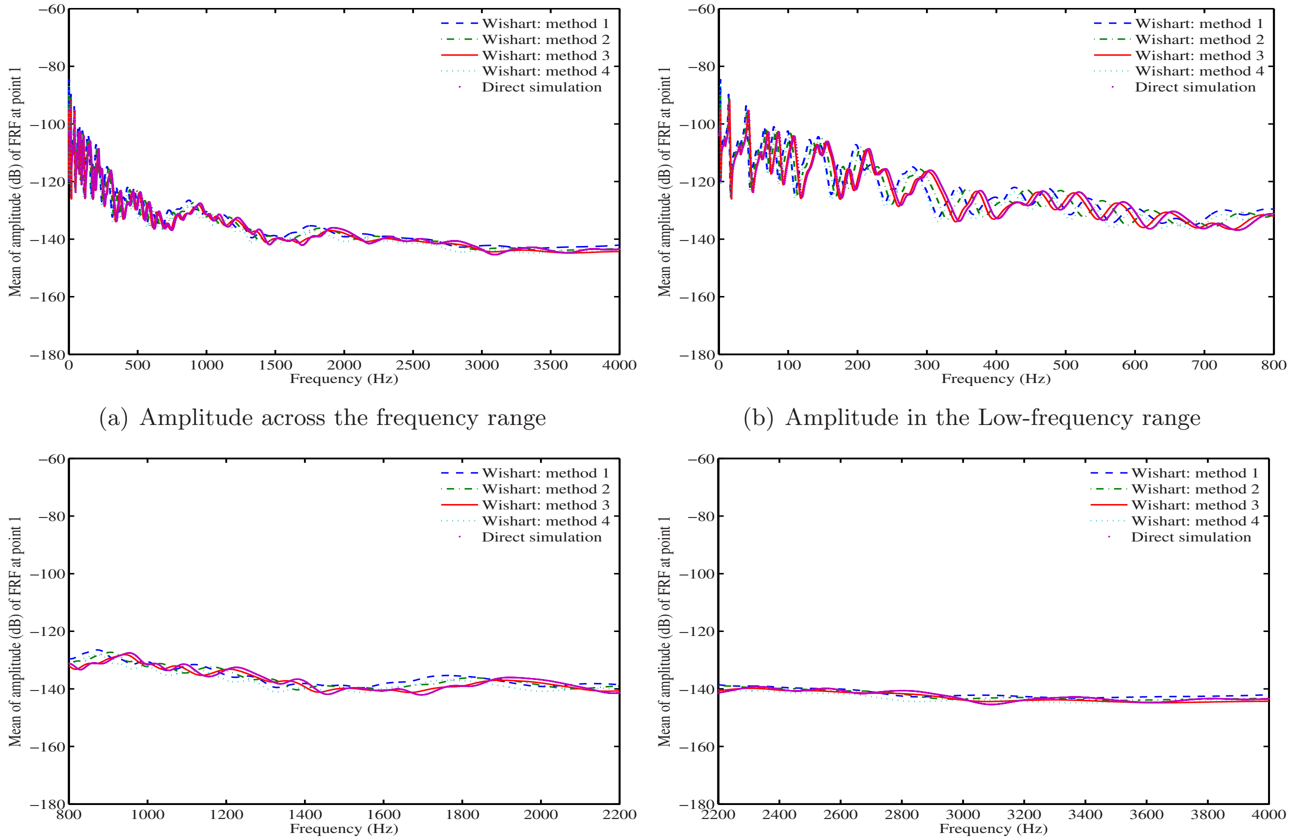

(a) Amplitude across the frequency range

(b) Amplitude in the Low-frequency range

(c) Amplitude in the Medium-frequency range

(d) Amplitude in the High-frequency range

Fig. 3. Comparison of the mean of the amplitude of the driving-point FRF obtained using the direct stochastic finite-element simulation and proposed four Wishart matrix approaches for the plate with randomly inhomogeneous material properties

mean matrix, produces the least error across the frequency range. Again, Approach 3 is significantly more accurate in the low-frequency region compared to the other approaches. From these results, we conclude that the Wishart random matrix corresponding to Approach 3 should be used for a system with parametric uncertainty. In the next section, we discuss the same system with nonparametric uncertainty.

Plate with Randomly Attached Spring-Mass Oscillators

In this example, we consider the same plate but with nonparametric uncertainty. We assume that 10 spring mass oscillators with random natural frequencies are attached at random nodal points in the plate. The nature of uncertainty in this case is different from the previous case because here the sparsity structure of the system matrices changes with different realizations of the system. For numerical calculations, we consider that the natural frequencies of the attached oscillators follow a uniform distribution between 0.2 and 4.0 kHz. A 1,000-sample Monte Carlo simulation is performed to obtain the FRFs.

From the simulated random mass and stiffness matrices we obtain $n=1{,}200$, $\sigma_M=0.13257$, and $\sigma_K=0.33349$. Since a 2% constant modal damping factor is assumed for all the modes, $\sigma_C=0$. The *only* uncertainty related information used in the random matrix approach are the values of σ_M and σ_K. The information regarding the location and natural frequencies of the attached oscillators are *not* used in the Wishart matrix approach. This is aimed to depict a realistic situation when the detailed information regarding uncertainties in a complex engineering system is not available to the analyst. Using $n=1{,}200$, $\sigma_M=0.13257$, and $\sigma_K=0.33349$, together with the deterministic values of **M** and **K**, from Eq. (31) we obtain

$$\theta_M = 18{,}184 \text{ and } \theta_K = 1{,}703 \tag{39}$$

Using these, the samples of the mass and stiffness matrices are simulated following the procedure outlined before.

The predicted mean of the amplitude using the direct stochastic finite-element simulation and four Wishart matrix approaches are compared in Fig. 7 for the cross-FRF. In Figs. 7(b–d), we have separately shown the low-, medium-, and high-frequency response, obtained by zooming in the appropriate frequency ranges in Fig. 7(a). The same frequency boundaries used in the previous example are used for this example also.

In Fig. 8, percentage errors in the mean of the amplitude of the cross-FRF obtained using the proposed four Wishart matrix approaches are shown. Again, percentage errors are calculated using the direct Monte Carlo simulation results as the benchmarks. An error using any one the random matrix approaches reduces with the increase in the frequency. Like the previous example with parametric uncertainty among the four Wishart matrix approaches, Approach 3 produces the least error across the frequency range. Approach 3 is also significantly more accurate in the low-frequency region compared to the other approaches.

The predicted standard deviation of the amplitude using the direct stochastic finite-element simulation and four Wishart matrix approaches are compared in Fig. 9 for the cross-FRF. In

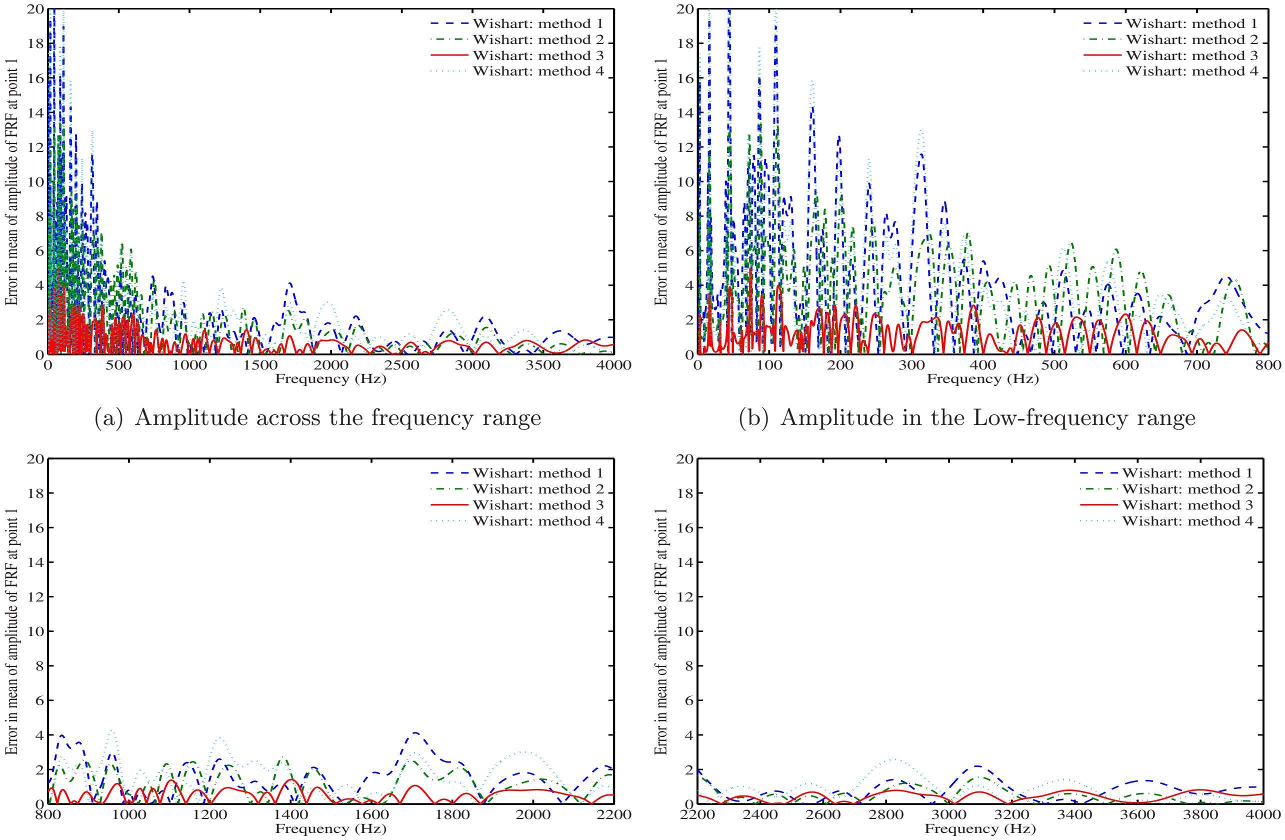

(a) Amplitude across the frequency range

(b) Amplitude in the Low-frequency range

(c) Amplitude in the Medium-frequency range

(d) Amplitude in the High-frequency range

Fig. 4. Comparison of percentage errors in the mean of the amplitude of the driving-point FRF obtained using the proposed four Wishart matrix approaches for the plate with randomly inhomogeneous material properties

Figs. 9(b–d), we have separately shown the low-, medium-, and high-frequency response, obtained by zooming in the appropriate frequency ranges in Fig. 9(a).

In Fig. 10, percentage errors in the standard deviation of the amplitude of the cross-FRF obtained using the proposed four Wishart matrix approaches are shown. Like the mean, error in standard deviation using any one of the random matrix approaches reduces with the increase in the frequency. Again, Approach 3 produces the least error across the frequency range. Approach 3 is also significantly more accurate in the low-frequency region compared to the other approaches. From these results, we conclude that the Wishart random matrix corresponding to Approach 3 should be used for a system with either parametric or nonparametric uncertainty.

Summary and Conclusions

When uncertainties in the system parameters and modeling are considered, the discretized equation of motion of linear dynamical systems is characterized by random mass, stiffness, and damping matrices. The possibility of using a Wishart random matrix model for the system matrices is investigated in the paper. The main conclusions are:

- For large system matrices, Wishart and gamma random matrices are similar. Wishart matrices are computationally more efficient to simulate compared to gamma random matrices since they are simply the product of a Gaussian random matrix and its transpose. As a result, the Wishart random matrix is recommended for all practical structural dynamic applications where system matrices are expected to be large.
- A wishart random matrix distribution can be obtained either using the maximum entropy approach or using the matrix factorization approach.
- The current maximum entropy approach gives a natural selection for the parameters. Through a numerical example it was shown that the parameters obtained using the maximum entropy approach may yield nonphysical results. In that, the "mean of the inverse" and the "inverse of the mean" of the random matrices can be significantly different.
- The parameters of the pdf of a Wishart random matrix obtained using the maximum entropy approach are not unique since they depend on what constraints are used in the optimization approach.
- Considering that the available "data" are the mean and (normalized) standard deviation of a system matrix, four different approaches are compared to identify the parameters of the Wishart distribution. It is shown that when the mean of the inverse is equal to the inverse of the mean of the system matrices, the calculated response statistics are in the best agreement with the direct numerical simulation results.
- Numerical results suggest that the difference between four proposed approaches are more in the low frequency regions and less in the higher frequency regions.

The derived Wishart random matrix model is applied to the forced vibration problem of a plate (with 1,200 degrees of freedom) with

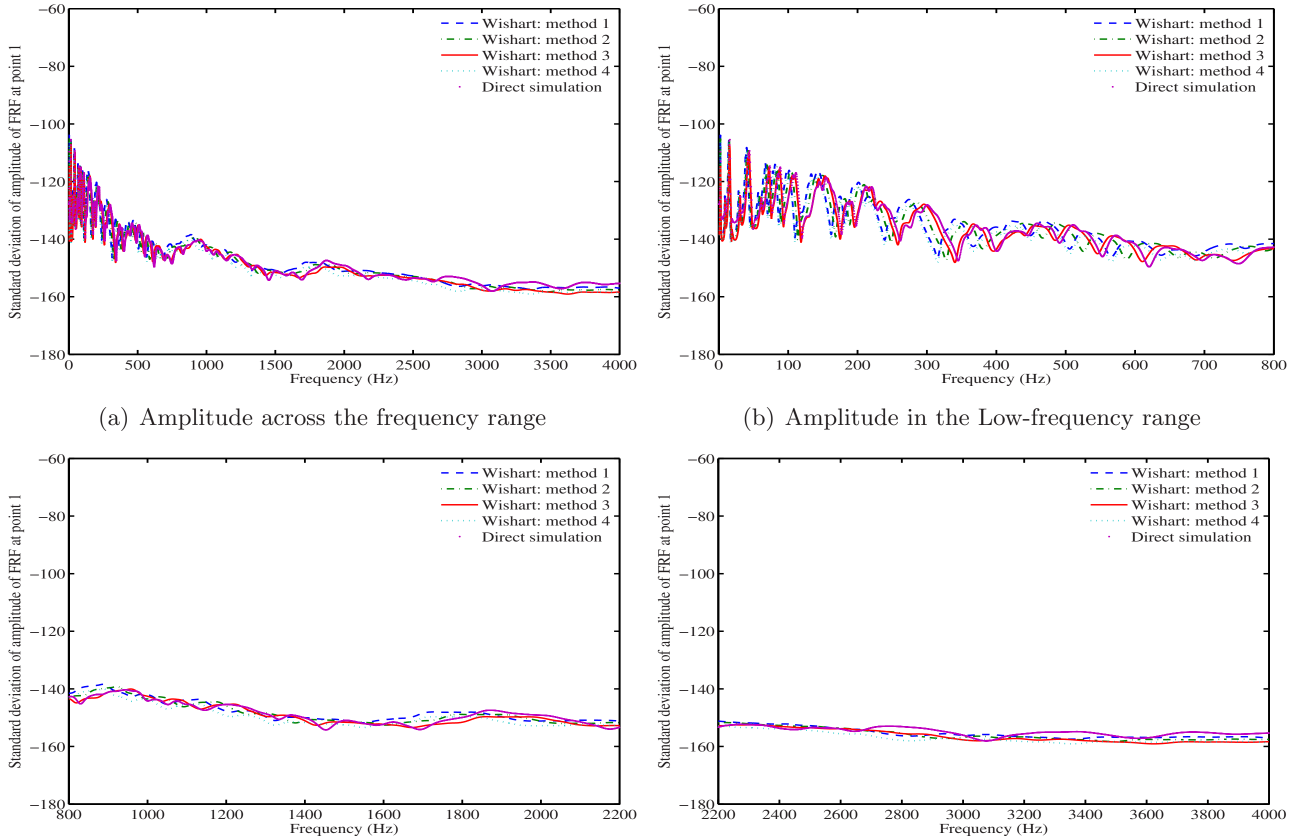

(a) Amplitude across the frequency range
(b) Amplitude in the Low-frequency range
(c) Amplitude in the Medium-frequency range
(d) Amplitude in the High-frequency range

Fig. 5. Comparison of the standard deviation of the amplitude of the driving-point FRF obtained using the direct stochastic finite-element simulation and proposed four Wishart matrix approaches for the plate with randomly inhomogeneous material properties

stochastically inhomogeneous properties and randomly attached oscillators. For both cases, it is possible to predict the variation of the dynamic response using the Wishart matrices across a wide range of driving frequency. These results suggest that a Wishart matrix with suggested parameters may be used as a consistent and unified uncertainty quantification tool valid for medium- and high-frequency vibration problems.

Acknowledgments

The writer acknowledges the financial support from the Royal Society, London and Engineering and Physical Sciences Research Council (U.K.) (EPSRC) through the award of an advanced research fellowship.

Appendix I. Wishart Distribution Using Matrix Factorization Approach

Suppose the matrix variate probability density function of $\mathbf{X} \in \mathbb{R}^{n\times p}$ is given by $p_{\mathbf{X}}(\mathbf{X})$: $\mathbb{R}^{n\times p} \to \mathbb{R}$. We have the following information and constraints to obtain $p_{\mathbf{X}}(\mathbf{X})$:

$$\int_{\mathbf{X}\in\mathbb{R}^{n\times p}} p_{\mathbf{X}}(\mathbf{X})d\mathbf{X} = 1 \quad \text{(the normalization)} \tag{40}$$

$$\int_{\mathbf{X}\in\mathbb{R}^{n\times p}} \mathbf{X}p_{\mathbf{X}}(\mathbf{X})d\mathbf{X} = \mathbf{O} \quad \text{(the mean matrix)} \tag{41}$$

and

$$\int_{\mathbf{X}\in\mathbb{R}^{n\times p}} \mathbf{X}\otimes\mathbf{X}^T p_{\mathbf{X}}(\mathbf{X})d\mathbf{X} = \mathbf{\Sigma}\otimes\mathbf{I}_p \quad \text{(the covariance matrix)} \tag{42}$$

The integrals appearing in the above three equations are $n\times p$ dimensional. Under these conditions, extending the standard maximum entropy argument to the random matrix case, it can be said that $\mathbf{X}$=Gaussian random matrix with mean $\mathbf{O}\in\mathbb{R}^{n\times p}$; $p\geqslant n$; and covariance $\mathbf{\Sigma}\otimes\mathbf{I}_p\in\mathbb{R}^{np\times np}$. Since $\mathbf{X}\sim N_{n,p}$ $(\mathbf{O},\mathbf{\Sigma}\otimes\mathbf{I}_p)$, the probability density function of the random matrix $\mathbf{X}$ can be obtained from Eq. (2) as

$$p_{\mathbf{X}}(\mathbf{X}) = (2\pi)^{-np/2}|\mathbf{\Sigma}|^{-p/2}\,\mathrm{etr}\left\{-\frac{1}{2}\mathbf{\Sigma}^{-1}\mathbf{X}\mathbf{X}^T\right\} \tag{43}$$

We first derive the matrix variate characteristic function of $\mathbf{G}=\mathbf{X}\mathbf{X}^T$ as

$$\phi_{\mathbf{G}}(\mathbf{Z}) = \mathrm{E}[\mathrm{etr}\{-\mathbf{Z}\mathbf{G}\}] = \mathrm{E}[\mathrm{etr}\{-\mathbf{Z}\mathbf{X}\mathbf{X}^T\}] \tag{44}$$

where $\mathbf{Z}=n\times n$ symmetric complex matrix. Using the probability density function of $\mathbf{X}$ in Eq. (43) we have

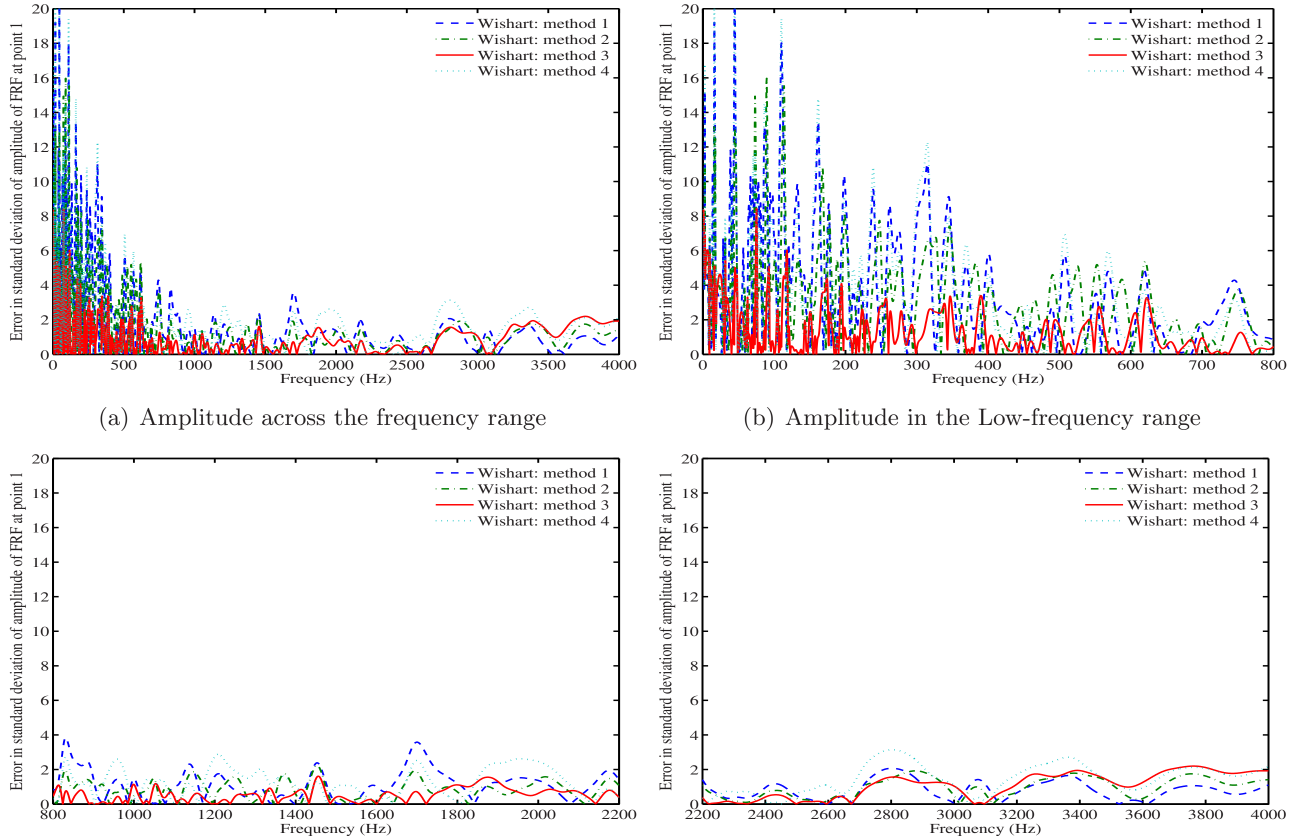

(a) Amplitude across the frequency range

(b) Amplitude in the Low-frequency range

(c) Amplitude in the Medium-frequency range

(d) Amplitude in the High-frequency range

Fig. 6. Comparison of percentage errors in the standard deviation of the amplitude of the driving-point FRF obtained using the proposed four Wishart matrix approaches for the plate with randomly inhomogeneous material properties

$$\begin{aligned}\phi_{\mathbf{G}}(\mathbf{Z}) &= (2\pi)^{-np/2}|\boldsymbol{\Sigma}|^{-p/2}\int_{\mathbb{R}_{n,p}} \operatorname{etr}\left\{-\mathbf{Z}\mathbf{X}\mathbf{X}^T - \frac{1}{2}\boldsymbol{\Sigma}^{-1}\mathbf{X}\mathbf{X}^T\right\}d\mathbf{X} \\ &= (2\pi)^{-np/2}|\boldsymbol{\Sigma}|^{-p/2}\int_{\mathbb{R}_{n,p}} \operatorname{etr}\left\{-\frac{1}{2}[\boldsymbol{\Sigma}^{-1} + 2\mathbf{Z}]\mathbf{X}\mathbf{X}^T\right\}d\mathbf{X}\end{aligned} \tag{45}$$

The domain of the above integral is the space of all $n \times p$ real matrices. This integral can be rearranged to obtain

$$\begin{aligned}\phi_{\mathbf{G}}(\mathbf{Z}) &= (2\pi)^{-np/2}|\boldsymbol{\Sigma}|^{-p/2} \\ &\times \int_{\mathbb{R}_{n,p}} \operatorname{etr}\left\{-\frac{1}{2}[\boldsymbol{\Sigma}^{-1} + 2\mathbf{Z}]^{1/2}\mathbf{X}\mathbf{X}^T[\boldsymbol{\Sigma}^{-1} + 2\mathbf{Z}]^{1/2}\right\}d\mathbf{X}\end{aligned} \tag{46}$$

We use a linear transformation

$$\mathbf{X} = [\boldsymbol{\Sigma}^{-1} + 2\mathbf{Z}]^{-1/2}\mathbf{Y} \tag{47}$$

The Jacobian associated with the above transformation can be obtained as

$$d\mathbf{X} = |\boldsymbol{\Sigma}^{-1} + 2\mathbf{Z}|^{-p/2}d\mathbf{Y} \tag{48}$$

Substituting $\mathbf{X}$ and $d\mathbf{X}$ from Eqs. (47) and (48) into Eq. (46), one has

$$\begin{aligned}\phi_{\mathbf{G}}(\mathbf{Z}) &= (2\pi)^{-np/2}|\boldsymbol{\Sigma}|^{-p/2}\int_{\mathbb{R}_{n,p}} \operatorname{etr}\left\{-\frac{1}{2}\mathbf{Y}\mathbf{Y}^T\right\}|\boldsymbol{\Sigma}^{-1} + 2\mathbf{Z}|^{-p/2}d\mathbf{Y} \\ &= |\mathbf{I}_n + 2\mathbf{Z}\boldsymbol{\Sigma}|^{-p/2}\left((2\pi)^{-np/2}\int_{\mathbb{R}_{n,p}} \operatorname{etr}\left\{-\frac{1}{2}\mathbf{Y}\mathbf{Y}^T\right\}d\mathbf{Y}\right)\end{aligned} \tag{49}$$

The second part of the above equation is the integration of the probability density function of a $n \times p$ Gaussian random matrix with zero mean and unit covariance [a special case of Eq. (2)]. Therefore

$$(2\pi)^{-np/2}\int_{\mathbb{R}_{n,p}} \operatorname{etr}\left\{-\frac{1}{2}\mathbf{Y}\mathbf{Y}^T\right\}d\mathbf{Y} = 1 \tag{50}$$

and consequently

$$\phi_{\mathbf{G}}(\mathbf{Z}) = |\mathbf{I}_n + 2\mathbf{Z}\boldsymbol{\Sigma}|^{-p/2} \tag{51}$$

If $\mathbf{G}$ were $W_n(p, \boldsymbol{\Sigma})$, then the probability density function would have been given by

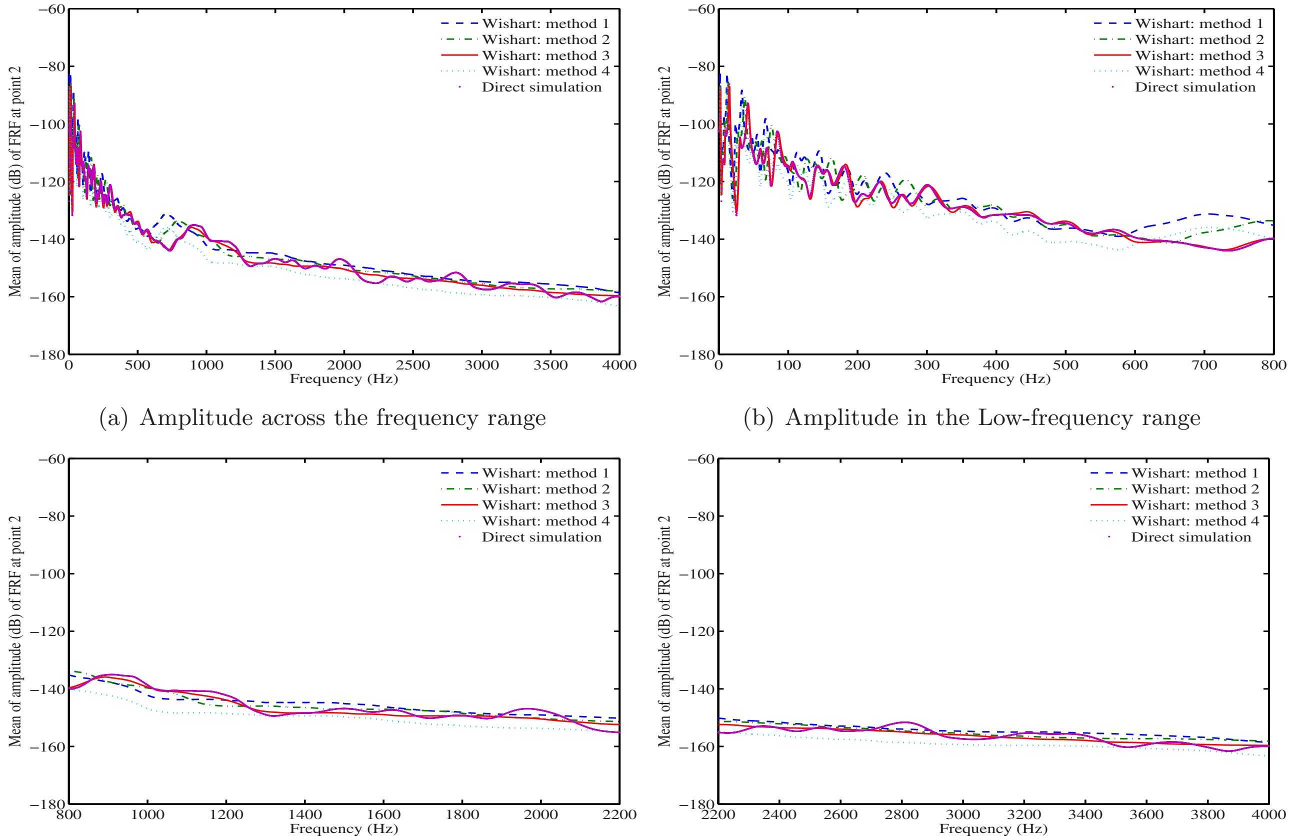

(a) Amplitude across the frequency range

(b) Amplitude in the Low-frequency range

(c) Amplitude in the Medium-frequency range

(d) Amplitude in the High-frequency range

Fig. 7. Comparison of the mean of the amplitude of the cross-FRF obtained using the direct stochastic finite-element simulation and proposed four Wishart matrix approaches for the plate with randomly attached oscillators with random natural frequencies

$$p_{\mathbf{G}}(\mathbf{G}) = \left\{2^{(1/2)np}\Gamma_n\left(\frac{1}{2}p\right)|\boldsymbol{\Sigma}|^{(1/2)p}\right\}^{-1}|\mathbf{G}|^{(1/2)(p-n-1)}\,\mathrm{etr}\left\{-\frac{1}{2}\boldsymbol{\Sigma}^{-1}\mathbf{G}\right\} \tag{52}$$

Using this, the matrix variate characteristic function can be obtained as

$$\phi_{\mathbf{G}}(\mathbf{Z}) = \mathrm{E}[\mathrm{etr}\{-\mathbf{ZG}\}] = \int_{\mathbf{G}>0} \mathrm{etr}\{-\mathbf{ZG}\}p_{\mathbf{G}}(\mathbf{G})d\mathbf{G} \tag{53}$$

$$= \left\{2^{(1/2)np}\Gamma_n\left(\frac{1}{2}p\right)|\boldsymbol{\Sigma}|^{(1/2)p}\right\}^{-1}\int_{\mathbf{G}>0} \mathrm{etr}\left\{-\mathbf{ZG}-\frac{1}{2}\boldsymbol{\Sigma}^{-1}\mathbf{G}\right\} \times|\mathbf{G}|^{(1/2)(p-n-1)}d\mathbf{G} \tag{54}$$

$$= \left\{2^{(1/2)np}\Gamma_n\left(\frac{1}{2}p\right)|\boldsymbol{\Sigma}|^{(1/2)p}\right\}^{-1} \times\int_{\mathbf{G}>0} \mathrm{etr}\left\{-\frac{1}{2}(\mathbf{I}_n+2\mathbf{Z}\boldsymbol{\Sigma})\boldsymbol{\Sigma}^{-1}\mathbf{G}\right\}|\mathbf{G}|^{\{p/2-(n+1)/2\}}d\mathbf{G} \tag{55}$$

The $n(n+1)/2$ dimensional integral appearing in the second part of the above equation can be evaluated exactly as

$$\begin{aligned}\int_{\mathbf{G}>0} \mathrm{etr}\left\{-\frac{1}{2}(\mathbf{I}_n+2\mathbf{Z}\boldsymbol{\Sigma})\boldsymbol{\Sigma}^{-1}\mathbf{G}\right\}|\mathbf{G}|^{\{p/2-(n+1)/2\}}d\mathbf{G} &= \left|\frac{1}{2}(\mathbf{I}_n+2\mathbf{Z}\boldsymbol{\Sigma})\boldsymbol{\Sigma}^{-1}\right|^{-p/2}\Gamma_n\left(\frac{1}{2}p\right)\\ &= 2^{(1/2)np}|(\mathbf{I}_n+2\mathbf{Z}\boldsymbol{\Sigma})|^{-p/2}|\boldsymbol{\Sigma}|^{(1/2)p}\Gamma_n\left(\frac{1}{2}p\right)\end{aligned} \tag{56}$$

Using this and simplifying Equation (55), we have

$$\phi_{\mathbf{G}}(\mathbf{Z}) = |\mathbf{I}_n+2\mathbf{Z}\boldsymbol{\Sigma}|^{-p/2} \tag{57}$$

Comparing this with Eq. (51) and using the uniqueness of the Laplace transform pairs of matrix variables, we say that the pdf of $\mathbf{G}$ follows the Wishart distribution given in Eq. (5).

Appendix II. Parameters for Optimal Wishart Distribution

Since $\mathbf{G}\sim W_n(p,\boldsymbol{\Sigma})$, there are two unknown parameters in this distribution, namely, p and $\boldsymbol{\Sigma}$. This implies that there are in total

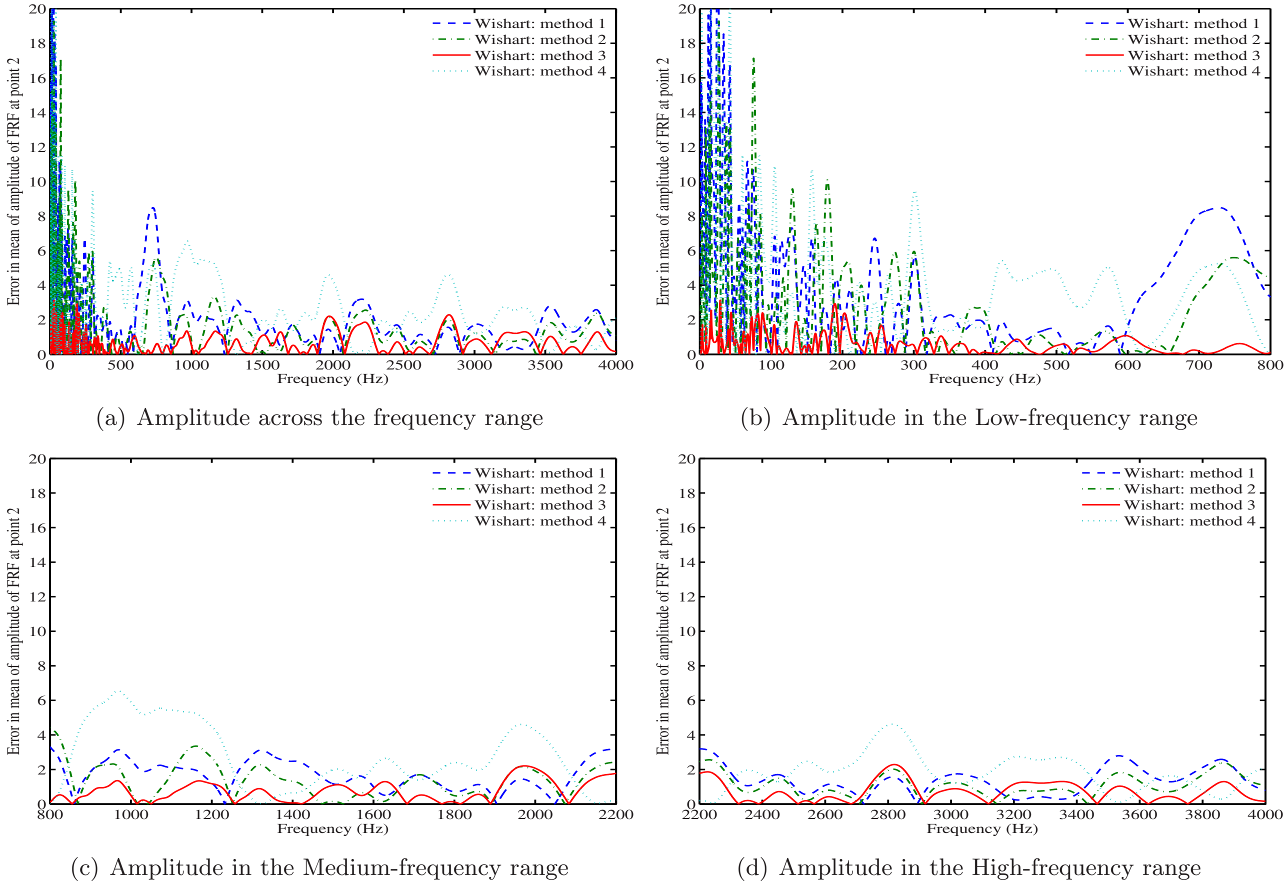

(a) Amplitude across the frequency range
(b) Amplitude in the Low-frequency range
(c) Amplitude in the Medium-frequency range
(d) Amplitude in the High-frequency range

Fig. 8. Comparison of percentage errors in the mean of the amplitude of the cross-FRF obtained using the proposed four Wishart matrix approaches for the plate with randomly attached oscillators with random natural frequencies

$1+n(n+1)/2$ number of unknowns as $\mathbf{\Sigma}$ is a $n\times n$ symmetric matrix. For the simplification of algebra, without any loss of generality we consider that

$$\mathbf{\Sigma}=\bar{\mathbf{G}}\mathbf{Y} \tag{58}$$

where $\mathbf{Y}\in\mathbb{R}^{n\times n}$=unknown matrix to be determined. Suppose that $\mathbf{G}$ has the Wishart distribution with parameters $p=n+1+\theta$ and $\mathbf{\Sigma}=\bar{\mathbf{G}}\mathbf{Y}$, that is, $\mathbf{G}\sim W_n\ (n+1+\theta,\bar{\mathbf{G}}\mathbf{Y})$. There are two undetermined parameters in the problem, namely, the scalar θ and the matrix $\mathbf{Y}$. The key idea is that the distribution of $\mathbf{G}$ must be such that $\mathrm{E}[\mathbf{G}]$ and $\mathrm{E}[\mathbf{G}^{-1}]$ be closest to $\bar{\mathbf{G}}$ and $\bar{\mathbf{G}}^{-1}$, respectively, in the least-squares sense.

The constant θ can be obtained from Eq. (21). This leaves us to determine only the matrix $\mathbf{Y}\in\mathbb{R}^{n\times n}$ such that $\mathrm{E}[\mathbf{G}]$ and $\mathrm{E}[\mathbf{G}^{-1}]$ become closest to $\bar{\mathbf{G}}$ and $\bar{\mathbf{G}}^{-1}$. Because $\mathbf{\Sigma}$ and $\bar{\mathbf{G}}$ are symmetric matrices, we have

$$\mathbf{\Sigma}=\mathbf{\Sigma}^T \quad \text{or} \quad \bar{\mathbf{G}}\mathbf{Y}=\mathbf{Y}^T\bar{\mathbf{G}} \quad \text{or} \quad \mathbf{Y}^T=\bar{\mathbf{G}}\mathbf{Y}\bar{\mathbf{G}}^{-1} \tag{59}$$

To obtain the optimal value of $\mathbf{Y}$ we define the "normalized errors" as

$$\boldsymbol{\varepsilon}_1=\|\bar{\mathbf{G}}-\mathrm{E}[\mathbf{G}]\|_{\mathrm{F}}/\|\bar{\mathbf{G}}\|_{\mathrm{F}} \tag{60}$$

$$\text{and} \quad \boldsymbol{\varepsilon}_2=\|\bar{\mathbf{G}}^{-1}-\mathrm{E}[\mathbf{G}^{-1}]\|_{\mathrm{F}}/\|\bar{\mathbf{G}}^{-1}\|_{\mathrm{F}} \tag{61}$$

Since $\mathbf{G}\sim W_n\ (n+1+\theta,\bar{\mathbf{G}}\mathbf{Y})$ we have

$$\mathrm{E}[\mathbf{G}]=(n+1+\theta)\bar{\mathbf{G}}\mathbf{Y} \tag{62}$$

$$\text{and} \quad \mathrm{E}[\mathbf{G}^{-1}]=\theta^{-1}\mathbf{Y}^{-1}\bar{\mathbf{G}}^{-1} \tag{63}$$

For any two compatible matrices we know that $\|\mathbf{AB}\|_{\mathrm{F}}=\|\mathbf{A}\|_{\mathrm{F}}\|\mathbf{B}\|_{\mathrm{F}}$ [see, for example, Horn and Johnson (1985), Chap. 5]. Using this, and substituting the expressions of $\mathrm{E}[\mathbf{G}]$ in Eq. (60), one obtains

$$\begin{aligned}\boldsymbol{\varepsilon}_1&=\|\bar{\mathbf{G}}-(n+1+\theta)\bar{\mathbf{G}}\mathbf{Y}\|_{\mathrm{F}}/\|\bar{\mathbf{G}}\|_{\mathrm{F}}=\|\bar{\mathbf{G}}(\mathbf{I}_n-(n+1+\theta)\mathbf{Y})\|_{\mathrm{F}}/\|\bar{\mathbf{G}}\|_{\mathrm{F}}\\&=\|\mathbf{I}_n-(n+1+\theta)\mathbf{Y}\|_{\mathrm{F}}\end{aligned} \tag{64}$$

Using the definition of the Frobenius norm, we have

$$\begin{aligned}\boldsymbol{\varepsilon}_1^2&=\mathrm{Trace}((\mathbf{I}_n-(n+1+\theta)\mathbf{Y})(\mathbf{I}_n-(n+1+\theta)\mathbf{Y})^T)\\&=\mathrm{Trace}(\mathbf{I}_n-(n+1+\theta)(\mathbf{Y}+\mathbf{Y}^T)+(n+1+\theta)^2\mathbf{Y}\mathbf{Y}^T)\end{aligned} \tag{65}$$

Substituting the expression of $\mathbf{Y}^T$ from Eq. (59), this equation can be expressed as

$$\begin{aligned}\boldsymbol{\varepsilon}_1^2&=\mathrm{Trace}(\mathbf{I}_n-(n+1+\theta)(\mathbf{Y}+\bar{\mathbf{G}}\mathbf{Y}\bar{\mathbf{G}}^{-1})+(n+1+\theta)^2\mathbf{Y}\bar{\mathbf{G}}\mathbf{Y}\bar{\mathbf{G}}^{-1})\\&=n-(n+1+\theta)\{\mathrm{Trace}(\mathbf{Y})+\mathrm{Trace}(\bar{\mathbf{G}}\mathbf{Y}\bar{\mathbf{G}}^{-1})\}\\&\quad+(n+1+\theta)^2\,\mathrm{Trace}(\mathbf{Y}\bar{\mathbf{G}}\mathbf{Y}\bar{\mathbf{G}}^{-1})\end{aligned} \tag{66}$$

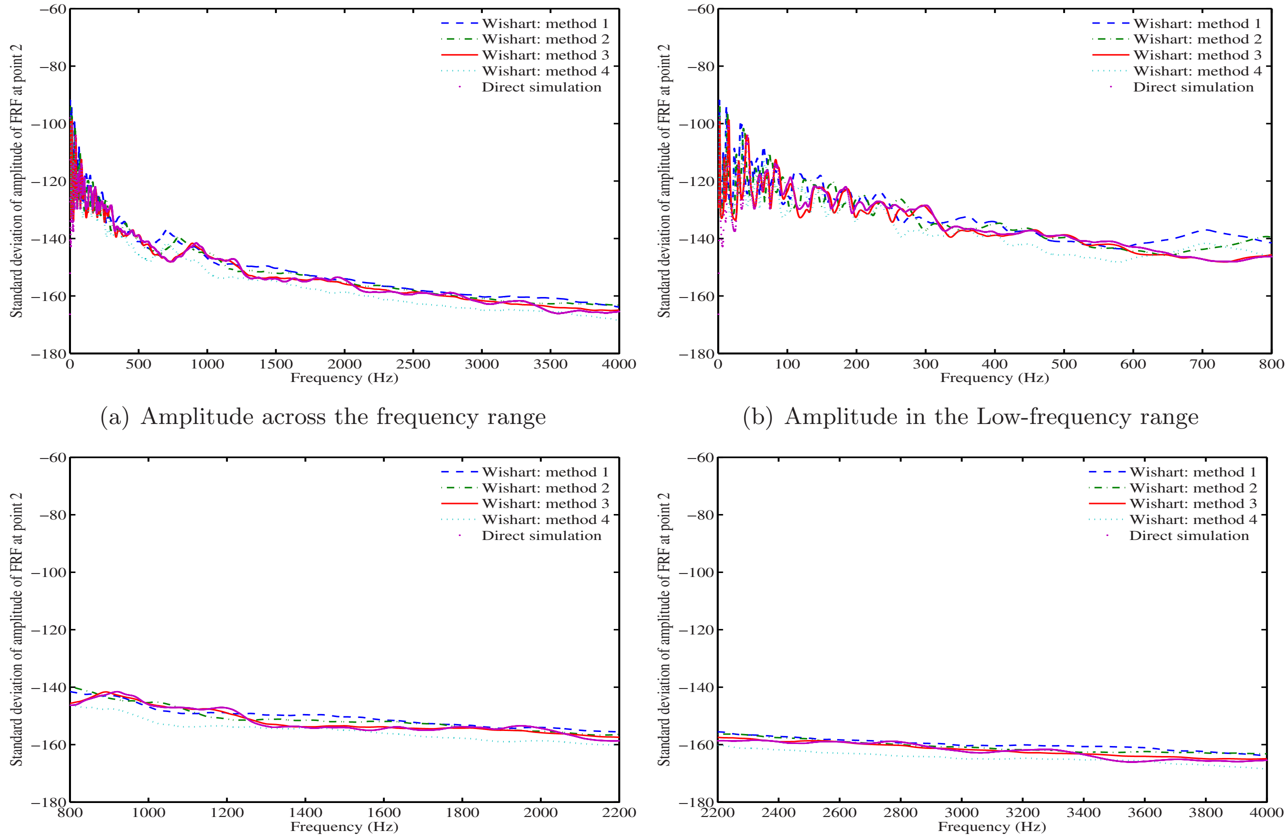

(a) Amplitude across the frequency range

(b) Amplitude in the Low-frequency range

(c) Amplitude in the Medium-frequency range

(d) Amplitude in the High-frequency range

Fig. 9. Comparison of the standard deviation of the amplitude of the cross-FRF obtained using the direct stochastic finite-element simulation and proposed four Wishart matrix approaches for the plate with randomly attached oscillators with random natural frequencies

Similarly, substituting the expressions of $\mathrm{E}[\mathbf{G}^{-1}]$ in Eq. (61), one can obtain

$$\boldsymbol{\varepsilon}_2 = \|\mathbf{I}_n - \theta^{-1}\mathbf{Y}^{-1}\|_{\mathrm{F}} \tag{67}$$

from which, noting that $\mathbf{Y}^{-T} = \bar{\mathbf{G}}^{-1}\mathbf{Y}^{-1}\bar{\mathbf{G}}$, we have

$$\begin{aligned}\boldsymbol{\varepsilon}_2^2 &= \mathrm{Trace}(\mathbf{I}_n - \theta^{-1}(\mathbf{Y}^{-1} + \mathbf{Y}^{-T}) + \theta^{-2}\mathbf{Y}^{-1}\mathbf{Y}^{-T})\\ &= \mathrm{Trace}(\mathbf{I}_n - \theta^{-1}(\mathbf{Y}^{-1} + \bar{\mathbf{G}}^{-1}\mathbf{Y}^{-1}\bar{\mathbf{G}}) + \theta^{-2}\mathbf{Y}^{-1}\bar{\mathbf{G}}^{-1}\mathbf{Y}^{-1}\bar{\mathbf{G}})\\ &= n - \theta^{-1}\{\mathrm{Trace}(\mathbf{Y}^{-1}) + \mathrm{Trace}(\bar{\mathbf{G}}^{-1}\mathbf{Y}^{-1}\bar{\mathbf{G}})\}\\ &\quad + \theta^{-2}\,\mathrm{Trace}(\mathbf{Y}^{-1}\mathbf{G}^{-1}\mathbf{Y}^{-1}\bar{\mathbf{G}})\end{aligned} \tag{68}$$

Now we define the objective function to be minimized as

$$\chi^2 = \boldsymbol{\varepsilon}_1^2 + \boldsymbol{\varepsilon}_2^2 \tag{69}$$

The optimal value of $\mathbf{Y}$ is obtained by setting

$$\frac{\partial\chi^2}{\partial\mathbf{Y}} = \mathbf{O} \quad \text{or} \quad \frac{\partial\boldsymbol{\varepsilon}_1^2}{\partial\mathbf{Y}} + \frac{\partial\boldsymbol{\varepsilon}_2^2}{\partial\mathbf{Y}} = \mathbf{O} \tag{70}$$

This expression has n^2 number of equations, which can be used to solve for $\mathbf{Y}$ uniquely, which has n^2 number of unknowns. To apply Eq. (70), we need to differentiate a scalar function with respect to a matrix. Differentiating Eq. (66) with respect to the matrix $\mathbf{Y}$, one has

$$\frac{\partial\boldsymbol{\varepsilon}_1^2}{\partial\mathbf{Y}} = -2(n+1+\theta)\mathbf{I}_n + (n+1+\theta)^2(\bar{\mathbf{G}}\mathbf{Y}\bar{\mathbf{G}}^{-1} + \bar{\mathbf{G}}^{-1}\mathbf{Y}\bar{\mathbf{G}})^T \tag{71}$$

Differentiating Eq. (68) with respect to the matrix $\mathbf{Y}$, we obtain

$$\frac{\partial\boldsymbol{\varepsilon}_2^2}{\partial\mathbf{Y}} = 2\theta^{-1}(\mathbf{Y}^{-2})^T - \theta^{-2}(\mathbf{Y}^{-1}\bar{\mathbf{G}}\mathbf{Y}^{-1}\bar{\mathbf{G}}^{-1}\mathbf{Y}^{-1} + \mathbf{Y}^{-1}\bar{\mathbf{G}}^{-1}\mathbf{Y}^{-1}\bar{\mathbf{G}}\mathbf{Y}^{-1})^T \tag{72}$$

Combining these two equations according to (70) and taking the transpose of the resulting equation, one obtains

$$\begin{aligned}&\mathbf{Y}^{-2} - \frac{1}{2}\theta^{-1}(\mathbf{Y}^{-1}\bar{\mathbf{G}}\mathbf{Y}^{-1}\bar{\mathbf{G}}^{-1}\mathbf{Y}^{-1} + \mathbf{Y}^{-1}\bar{\mathbf{G}}^{-1}\mathbf{Y}^{-1}\bar{\mathbf{G}}\mathbf{Y}^{-1})\\ &\quad - \theta(n+1+\theta)\mathbf{I}_n + \frac{1}{2}\theta(n+1+\theta)^2(\bar{\mathbf{G}}\mathbf{Y}\bar{\mathbf{G}}^{-1} + \bar{\mathbf{G}}^{-1}\mathbf{Y}\bar{\mathbf{G}}) = \mathbf{O}\end{aligned} \tag{73}$$

This is a nonlinear matrix equation of fourth order. Clearly,

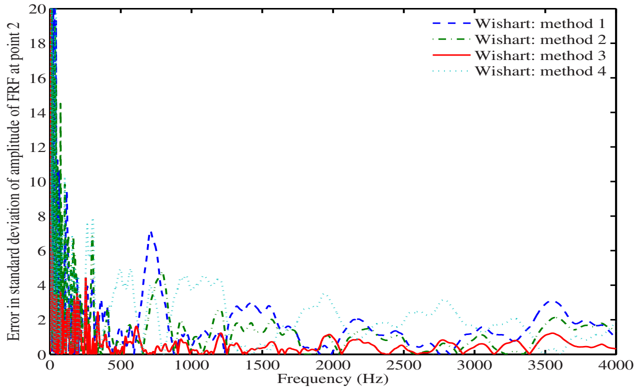

(a) Amplitude across the frequency range

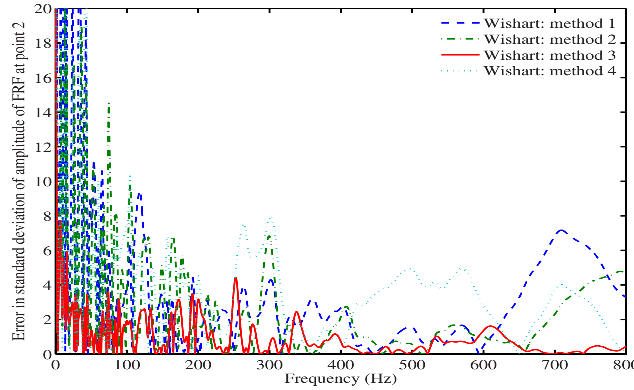

(b) Amplitude in the Low-frequency range

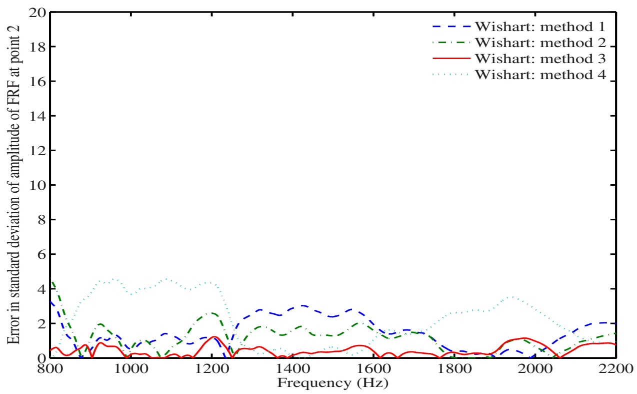

(c) Amplitude in the Medium-frequency range

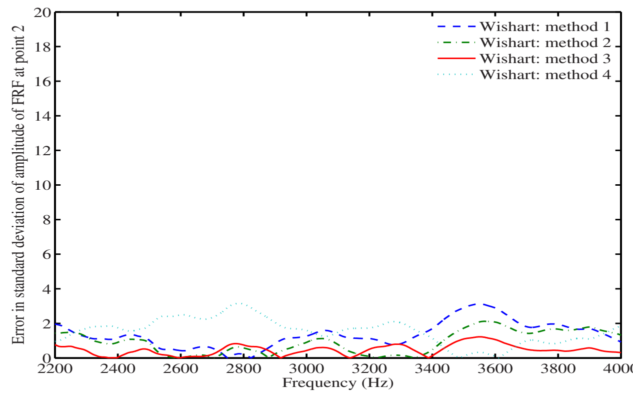

(d) Amplitude in the High-frequency range

Fig. 10. Comparison of percentage errors in the standard deviation of the amplitude of the cross-FRF obtained using the proposed four Wishart matrix approaches for the plate with randomly attached oscillators with random natural frequencies

there are more than one matrix solution to this equation. To obtain closed-from expressions of $\mathbf{Y}$, we try with a solution of the form

$$\mathbf{Y} = \alpha^{-1}\mathbf{I}_n \tag{74}$$

where α = positive real number to be determined. Substituting this in Eq. (73) and simplifying, one obtains the following scalar equation:

$$\alpha^4 - \theta\alpha^3 + \theta^2(n+1+\theta)\alpha - \theta^2(n+1+\theta)^2 = 0 \tag{75}$$

This fourth-order algebraic equation in α has the following four exact solutions

$$\alpha = \pm\sqrt{\theta(n+1+\theta)} \quad \text{and} \quad \alpha = \theta/2 \pm \mathrm{i}\sqrt{\theta(n+1+3\theta/4)} \tag{76}$$

Because α must be real and positive, the only feasible value of $\alpha \in \mathbb{R}^+$ is

$$\alpha = \sqrt{\theta(n+1+\theta)} \tag{77}$$

Therefore

$$\mathbf{Y} = \{\theta(n+1+\theta)\}^{-1/2}\mathbf{I}_n \tag{78}$$

Substituting this value of $\mathbf{Y}$ in Eq. (73), one can verify that this equation is satisfied *exactly* by the above solution. Using the expression of $\mathbf{Y}$ in Equation (78), we have

$$\mathbf{\Sigma} = \bar{\mathbf{G}}\mathbf{Y} = \{\theta(n+1+\theta)\}^{-1/2}\bar{\mathbf{G}} \tag{79}$$

This result implies that $\mathbf{G} \sim W_n\,(n+1+\theta, \bar{\mathbf{G}}/\sqrt{\theta(n+1+\theta)})$. For these parameter selections, the mean of $\mathbf{G}$ and $\mathbf{G}^{-1}$ become simultaneously closest to $\bar{\mathbf{G}}$ and $\bar{\mathbf{G}}^{-1}$.

Notation

The following symbols are used in this paper:

$\mathbf{B}_n$ = $n^2 \times n(n+1)/2$-dimensional translation matrix;
$\mathbb{C}$ = space of complex numbers;
$\mathbf{D}(\omega)$ = dynamic stiffness matrix;
$\mathrm{etr}\{\cdot\}$ = $\exp\{\mathrm{Trace}(\cdot)\}$;
$\mathbf{f}(t)$ = forcing vector;
$\mathbf{G}$ = symbol for a system matrix, $\mathbf{G} \equiv \{\mathbf{M}, \mathbf{C}, \mathbf{K}\}$;
$\mathbf{H}(\omega)$ = frequency response function (FRF) matrix;
$\mathbf{M}$, $\mathbf{C}$, and $\mathbf{K}$ = mass, damping, and stiffness matrices, respectively;
n = number of degrees of freedom;
$p, \mathbf{\Sigma}$ = scalar and matrix parameters of the Wishart distribution;
$p_{(\cdot)}(\mathbf{X})$ = probability density function of $(\cdot)$ in (matrix) variable $\mathbf{X}$;
$\mathbf{q}(t)$ = response vector;
$\mathbb{R}$ = space of real numbers;
$\mathbb{R}_n^+$ = space $n \times n$ real positive definite matrices;

$\mathbb{R}^{n\times m}$ = space $n\times m$ real matrices;
Trace$(\cdot)$ = sum of the diagonal elements of a matrix;
$\Gamma_n(a)$ = multivariate gamma function;
δ_{ij} = Kronecker's delta function;
ν = order of the inverse-moment constraint;
σ_G = normalized standard deviation of $\mathbf{G}$;
ω = excitation frequency;
$(\cdot)^\dagger$ = Moore-Penrose generalized inverse of a matrix;
$(\cdot)^T$ = matrix transposition;
$|\cdot|$ = determinant of a matrix;
$\otimes$ = Kronecker product [see Graham (1981)]; and
$\sim$ = distributed as.

References

Adhikari, S. (2007a). "Matrix variate distributions for probabilistic structural mechanics." *AIAA J.*, 45(7), 1748–1762.

Adhikari, S. (2007b). "On the quantification of damping model uncertainty." *J. Sound Vib.*, 305(1–2), 153–171.

Adhikari, S., and Manohar, C. S. (1999). "Dynamic analysis of framed structures with statistical uncertainties." *Int. J. Numer. Methods Eng.*, 44(8), 1157–1178.

Adhikari, S., and Manohar, C. S. (2000). "Transient dynamics of stochastically parametered beams." *J. Eng. Mech.*, 126(11), 1131–1140.

Cotoni, V., Shorter, P., and Langley, R. S. (2007). "Numerical and experimental validation of a hybrid finite element-statistical energy analysis method." *J. Acoust. Soc. Am.*, 122(1), 259–270.

Eaton, M. L. (1983). *Multivariate statistics: A vector space approach*, Wiley, New York.

Elishakoff, I., and Ren, Y. J. (2003). *Large variation finite element method for stochastic problems*, Oxford Univ. Press, Oxford, U.K.

Ghanem, R., and Spanos, P. (1991). *Stochastic finite elements: A spectral approach*, Springer, New York.

Girko, V. L. (1990). *Theory of random determinants*, Kluwer, The Netherlands.

Graham, A. (1981). *Kronecker products and matrix calculus with applications, mathematics and its applications*, Ellis Horwood Limited, Chichester, U.K.

Gupta, A., and Nagar, D. (2000). *Matrix variate distributions, monographs and surveys in pure and applied mathematics*, Chapman and Hall/CRC, London.

Haldar, A., and Mahadevan, S. (2000). *Reliability assessment using stochastic finite element analysis*, Wiley, New York.

Horn, R. A., and Johnson, C. R. (1985). *Matrix analysis*, Cambridge Univ. Press, Cambridge, U.K.

Janik, R. A., and Nowak, M. A. (2003). "Wishart and anti-wishart random matrices." *J. Phys. A*, 36(2), 3629–3637.

Johnson, N. L., Kotz, S., and Balakrishnan, N. (1994). *Continuous univariate distributions*, Vol. 1, Wiley Series in Probability and Mathematical Statistics, Wiley, New York.

Kleiber, M., and Hien, T. D. (1992). *The stochastic finite element method*, Wiley, Chichester, U.K.

Langley, R. S., and Bremner, P. (1999). "A hybrid method for the vibration analysis of complex structural-acoustic systems." *J. Acoust. Soc. Am.*, 105(3), 1657–1671.

Langley, R. S., and Cotoni, V. (2007). "Response variance prediction for uncertain vibro-acoustic systems using a hybrid deterministic-statistical method." *J. Acoust. Soc. Am.*, 122(6), 3445–3463.

Lyon, R. H., and Dejong, R. G. (1995). *Theory and application of statistical energy analysis*, 2nd Ed., Butterworth-Heinmann, Boston.

Manohar, C. S., and Adhikari, S. (1998a). "Dynamic stiffness of randomly parametered beams." *Probab. Eng. Mech.*, 13(1), 39–51.

Manohar, C. S., and Adhikari, S. (1998b). "Statistical analysis of vibration energy flow in randomly parametered trusses." *J. Sound Vib.*, 217(1), 43–74.

Mathai, A. M. (1997). *Jocobians of matrix transformation and functions of matrix arguments*, World Scientific, London.

Mathai, A. M., and Provost, S. B. (1992). *Quadratic forms in random variables: Theory and applications*, Marcel Dekker, New York.

Matthies, H. G., Brenner, C. E., Bucher, C. G., and Soares, C. G. (1997). "Uncertainties in probabilistic numerical analysis of structures and solids—Stochastic finite elements." *Struct. Safety*, 19(3), 283–336.

Mehta, M. L. (1991). *Random matrices*, 2nd Ed., Academic Press, San Diego.

Mezzadri, F., and Snaith, N. C., eds. (2005). *Recent perspectives in random matrix theory and number theory*, London Mathematical Society Lecture Note, Cambridge Univ. Press, Cambridge, U.K.

Muirhead, R. J. (1982). *Aspects of multivariate statistical theory*, Wiley, New York.

Nair, P. B., and Keane, A. J. (2002). "Stochastic reduced basis methods." *AIAA J.*, 40(8), 1653–1664.

Sachdeva, S. K., Nair, P. B., and Keane, A. J. (2006a). "Comparative study of projection schemes for stochastic finite element analysis." *Comput. Methods Appl. Mech. Eng.*, 195(19–22), 2371–2392.

Sachdeva, S. K., Nair, P. B., and Keane, A. J. (2006b). "Hybridization of stochastic reduced basis methods with polynomial chaos expansions." *Probab. Eng. Mech.*, 21(2), 182–192.

Sarkar, A., and Ghanem, R. (2002). "Mid-frequency structural dynamics with parameter uncertainty." *Comput. Methods Appl. Mech. Eng.*, 191(47–48), 5499–5513.

Sarkar, A., and Ghanem, R. (2003a). "Reduced models for the medium-frequency dynamics of stochastic systems." *J. Acoust. Soc. Am.*, 113(2), 834–846.

Sarkar, A., and Ghanem, R. (2003b). "A substructure approach for the midfrequency vibration of stochastic systems." *J. Acoust. Soc. Am.*, 113(4), 1922–1934.

Shinozuka, M., and Yamazaki, F. (1998). "Stochastic finite element analysis: An introduction." *Stochastic structural dynamics: Progress in theory and applications*, S. T. Ariaratnam, G. I. Schuëller, and I. Elishakoff, eds., Elsevier Applied Science, London.

Soize, C. (2000). "A nonparametric model of random uncertainties for reduced matrix models in structural dynamics." *Probab. Eng. Mech.*, 15(3), 277–294.

Soize, C. (2001). "Maximum entropy approach for modeling random uncertainties in transient elastodynamics." *J. Acoust. Soc. Am.*, 109(5), 1979–1996.

Sudret, B., and Der-Kiureghian, A. (2000). "Stochastic finite element methods and reliability," *Rep. No. UCB/SEMM-2000/08*, Dept. of Civil and Environmental Engineering, Univ. Of California, Berkeley, Berkeley, Calif.

Tulino, A. M., and Verdú, S. (2004). *Random matrix theory and wireless communications*, Now Publishers Inc., Hanover, Mass.

Wigner, E. P. (1958). "On the distribution of the roots of certain symmetric matrices." *Ann. Math.*, 67(2), 325–327.

Wishart, J. (1928). "The generalized product moment distribution in samples from a normal multivariate population." *Biometrika*, 20(A), 32–52.